Effect of Cutting Parameters on Micro Drilling Characteristics of Incoloy 825

Sabana Azim

Department of Mechanical Engineering

National Institute of Technology Rourkela

Effect of Cutting Parameters on Micro Drilling Characteristics of Incoloy 825

Dissertation submitted in partial fulfilment

of the requirements of the degree of

Master of Technology

in

Mechanical Engineering

by

Sabana Azim

(Roll number: 214ME2547)

based on research carried out

under the supervision of

Dr. S. Gangopadhyay

May, 2016

Department of Mechanical Engineering

National Institute of Technology Rourkela

Department of Mechanical Engineering

National Institute of Technology Rourkela

Supervisors' Certificate

This is to certify that the work presented in this dissertation entitled "*Effect of Cutting Parameters on Micro Drilling Characteristics of Incoloy 825 "* by "*Sabana Azim*, Roll Number 214ME2547, is a record of original research carried out by her under our supervision and guidance in partial fulfilment of the requirements of the degree of *Master of Technology* in *Mechanical Engineering*. Neither this dissertation nor any part of it has been submitted for any degree or diploma to any institute or university in India or abroad.

May 24, 2016

NIT Rourkela

Dr. S. Gangopadhyay

Assistant Professor

Department of Mechanical Engineering

NIT Rourkela

Declaration of Originality

I, *Sabana Azim*, Roll Number 214ME2547 hereby declare that this dissertation entitled *Effect of Cutting Parameters on Micro Drilling Characteristics of Incoloy 825* presents my original work carried out as a masters student of NIT Rourkela and, to the best of my knowledge, contains no material previously published or written by another person, nor any material presented by me for the award of any degree or diploma of NIT Rourkela or any other institution. Any contribution made to this research by others, with whom I have worked at NIT Rourkela or elsewhere, is explicitly acknowledged in the dissertation. Works of other authors cited in this dissertation have been duly acknowledged under the sections "Reference". I have also submitted my original research records to the scrutiny committee for evaluation of my dissertation.

I am fully aware that in case of any non-compliance detected in future, the Senate of NIT Rourkela may withdraw the degree awarded to me on the basis of the present dissertation.

May 24, 2016

NIT Rourkela *Sabana Azim*

Acknowledgement

I would like to express my gratitude to my supervisor **Prof. S. Gangopadhyay** for his invaluable guidance, constant motivation and kind co-operation which has been instrumental in the success of this thesis.

I am extremely thankful to **Prof. S. S. Mahapatra,** Head of the Department, Mechanical Engineering, for providing invaluable departmental facilities. I would also take this opportunity to thank **Mr. Arabinda Khuntia,** Technical Assistant of Production Engineering Laboratory and Department of Mechanical Engineering for carrying out my experimental work. I also express my sincere thanks to the staff members of Mechanical Engineering Department office for their timely help and prompt response. Last but not the least; I wish to express my sincere thanks to the faculty of IIT Bombay **Prof. Ramesh Singh** and the research scholars **S. Anandita** and **Rinku Mittal** who provided with necessary facilities at various stages of this work without which experimental work would not have been possible.

I would also like to express my special thanks to my co-researchers **Aruna Thakur, Gangadharudu Talla, Arun Jacob, Roshin Thomas Varughese** and **Mahendra Singh** for their constant help and advice throughout and for successful completion of my experiments and thesis. Many friends have helped me stay sane through these difficult years. Their support and care helped me overcome setbacks and stay focused on my research work. I greatly value their friendship and I deeply appreciate their belief in me.

May 21, 2016
NIT Rourkela

Sabana Azim
Roll Number: 214ME2547

ABSTRACT

The study focuses on the micro drilling of Incoloy 825 alloy under flood cutting condition. Micro drilling on nickel based superalloy is very challenging process due to the material properties, operating conditions, low thermal conductivity and high quality requirements. Due to low thermal conductivity of material heat is concentrated near tool tip and unable to dissipate for which tool wear occurs. The current study described the machinability of Incoloy 825 in micro drilling operation and also the effect of spindle rpm and feed rate on thrust force, torque, radial component force, tangential component forces, oversize diameter and white layer thickness. The current study investigates the influence of micro drilling parameters on surface profile and circumferential damage of micro holes (in terms of damaged layer thickness). ANSYS simulation was carried out to theoretically determine and evaluated necessary data like equivalent stress and deformation. Statistical analysis was also carried out to develop predictive models for various output characteristics.

Keywords: Incoloy 825; Micro drilling; White layer; Surface roughness; Oversize error; Simulation, Statistical analysis

Contents

Supervisors Certificate **III**

Declaration of Originality **IV**

Acknowledgment **V**

Abstract **VI**

List of Figures **IX**

List of Tables **XI**

Introduction 1

1.1 Ni-based super alloys 1

1.2 The forming of Ni-based super alloy 2

1.3 Application of superalloy in aerospace engine 3

1.4 Phases of Ni-based superalloys 3

1.5 Micro-structure of Ni-based superalloy 4

1.6 Incoloy 825 4

1.7 Applications of Incoloy 825 5

1.8 Micro machining 5

1.9 Classification of micro machining 6

1.10 Micro drilling 7

1.11 Applications of micro drilling: 9

Literature Review 10

2.1 Effect of machining parameters on micro drilling 10

2.2 Effect of environment on micro drilling 12

2.3 Effect on Surface Integrity during micro drilling 13

2.4 Modeling and simulation 14

2.5 Motivation and objectives 14

Experimental Details 16

3.1 Details of cutting tool 16

3.2 Workpiece Description 17

3.3 Selection of Cutting Parameters 18
3.4 Machining Performance Evaluation 20
Results and Discussions 26
4.1 Experimental Results 26
4.2 Simulation 31
4.3 Surface integrity 36
4.3.1 Surface roughness 36
4.3.2 Circumferential deformation layer 38
4.3.3 Oversize error of micro hole 42
4.3.4 Investigation on white layer formation 46
4.4 Predictive regression models 49
Conclusions 53
Future Scope of Work 54
References 55

List of Figures

Fig.1.1 Classification of micro machining 7
Fig.1.2: Micro drilling set up arrangement 8
Fig. 3.1: Carbide uncoated drill bit 16
Fig. 3.2: Ultra-high speed micro machine 20
Fig. 3.3: (a) Experimental set up (b) Charge amplifier and coolant set up 21
Fig. 3.4: Multi component dynamometer (KISTLER 9256 C1) 22
Fig. 3.5: Sample of Incoloy material after micro drilling 23
Fig. 3.6: Surface profile measurement setup 23
Fig.3.7: FESEM (field emission scanning electron microscopy) 24
Fig. 4.1: Variation of thrust force (Fz) with speed rpm and feed rate 26
Fig. 4.2: Variation of torque with speed rpm and feed rate 27
Fig. 4.3: Variation of radial force with speed rpm and feed rate 27
Fig. 4.4: Variation of radial force with speed rpm and feed rate 28
Fig. 4.5: Representative graph of thrust force (Fz) w.r.t time 29
Fig. 4.6: Representative graph of torque w.r.t time 29
Fig. 4.7: Variation of equivalent stress with speed rpm and feed rate 31
Fig. 4.8: Variation of deformation with speed rpm and feed rate 32
Fig. 4.9: Meshing of micro drill bit 32
Fig. 4.10: Representative image of deformation at condition (10000rpm and 12µm/rev)..33
Fig. 4.11: Total deformation in axial and diametric plane at condition (10000rpm, 12µm/rev) 33
Fig. 4.12: Representative image of equivalent stress at condition(10000rpm, 12µm/rev).34
Fig. 4.13: Maximum principal stress in axial and diametric plane at condition (10000 rpm, 12µm/rev) 34
Fig. 4.14: Representative image of surface profile 35

Fig. 4.15: Variation of surface roughness with speed rpm and feed rate 36
Fig. 4.16: Representative image circumferential deformation layer of drilled hole..... 37
Fig. 4.17: Representative images of circumferential deformation layer with different conditions..... 38,39
Fig. 4.18: Circumferential deformation layer with speed rpm and feed rate..... 40
Fig. 4.19: Representative image of micro drilled hole 41
Fig. 4.20: Representative images of micro drilled hole with different conditions 42,43
Fig. 4.21: Variation of oversize error with speed rpm and feed rate……...44
Fig. 4.22: Representative image of white layer……46
Fig. 4.23: Representative images of white layer at different speed rpm with lower and higher feed rate……47
Fig.4.24: Effect of speed rpm and feed rate on thrust force (F_z)……49
Fig.4.25: Effect of speed rpm and feed rate on radial force (F_x)……50
Fig.4.26: Effect of speed rpm and feed rate on radial force (F_y)……50
Fig.4.27: Effect of speed rpm and feed rate on torque……50
Fig.4.28: Effect of speed rpm and feed rate on surface roughness (R_a)……..51
Fig.4.29: Effect of speed rpm and feed rate on circumferential deformation layer……51
Fig.4.30: Effect of speed rpm and feed rate on oversize error……51

List of Tables

Table.3.1: Detail features of tool geometry 176
Table.3.2: Chemical composition of Incoloy 825 17
Table.3.3: Physical and mechanical properties of Incoloy 825 17
Table.3.4: Cutting Parameters 19
Table.3.5: Conditions for different holes 19
Table.3.6: Technical description of ultra high speed micro machine 20
Table.3.7: Specification of dynamometer (9256C1) 22
Table 4.1: Experimental forces and torque for micro drilling 25
Table.4.2: Simulation data of deformation and equivalent stress generated by micro drilling 30
Table.4.3: Surface roughness measurements for the micro holes 36
Table.4.4: Measured circumferential deformation layer of micro drilling……..40
Table.4.5: Measured Oversize error of micro drilling…….44
Table.4.6: Predicted values of output responses…….49

CHAPTER 1

Introduction

Machining is the important process that provides required shape to any workpiece by removing material in the form of chip. It is achieved as relative movement of any cutting tool w.r.t a workpiece in different direction either automatically or manually. This relative movement is achieved either by the motion of workpiece or tool or combination of both. Basically, machining is the finishing process by which any workpiece of required shape, size and finish is produce by continuous removal of extra metal from the workpiece in the form of chips by movement of cutting tool across its surface. Despite all this, a very important aspect has been observed in shape forming techniques, where machining is a primary activity performed in various industries. The machining system consists of a cutting tool, workpiece and machine. The cutting tool plays a very important role in setting the cutting parameters which depend upon the material of the cutting tool. Therefore the main reason behind machining is to explore the workpiece and tool interaction so as to get a proper set up of cutting parameter which helps improving the overall productivity of industries and also improvement of its quality. Some of the main factors which help to decide the machining characteristics of Ni-based super alloy are cutting tool life, cutting forces, MRR, surface roughness and surface integrity.

The term machinability is defined as ease with which a workpiece can be cut to desired shape, size in accordance to the machining operation involved. The machinability index is very much influenced by the properties and the geometry of the cutting tool, cutting parameter used, material properties being machined. The cutting parameters specifically include cutting environment, machine tool rigidity etc. The productivity of any machining operation can be improved by proper combination of cutting tool, machining parameter and machine tool.

1.1 Ni-based super alloys

Ni- based super alloys can withstand very high temperature and has properties like good corrosion and creep resistance, acid resistance, high thermal resistance to be used in the production of various components like frame works, valves, turbines, aviation and

military sector. It has been widely utilized to produce temperature resistance turbine blades. Many metallurgical application related to austenitic stainless steel particularly consist of Ni, Cr and Mo to enhance their resistance to corrosion. The name super alloys itself signify its outstanding high temperature strength and their resistance to oxidation. These superalloy consist a very balanced alloying elements like Co, Cr, Al, Ti as well as some other additives. They can sustain up to a temperature of 1000 ºC which exceeds ordinary steel at room temperature. They are very essential in manufacturing the hottest parts of gas turbine for power generation air craft.

1.2 The forming of Ni-based super alloy

Incoloy: Number of chemical processing industry utilized Incoloy in the manufacturing of evaporator tubes, steam, condenser and heater. It is also used in construction of nuclear reactor. These alloys are oxidation and corrosion resistance materials used in extreme environments. Incoloy high temperature strength is developed by solid solution strengthening method depending on the alloy. Incoloy has certain difficulty in machine by traditional technique as it under goes rapid work hardening. North American X-15 rocket powered air craft is made up of Incoloy alloy. Recently launched space X falcn 9 launch vehicle by ISRO uses Incoloy in the engine manifold. It has its extended application in 3D printing and laser printing.

Nimonic: It is a registered trademark of special metals corporation that refer to the family of Ni-based high temperature low creep super alloy. It consist of more than 50% of Ni and 20% of Cr. As well as some additives like Ti and Al. It is mainly used in gas turbine components and reciprocating internal engines.

Waspaloy: It is FCC Ni-based alloy which is typically used in high temperature processes like gas turbine; it is the hardened form of austenite. It consist of 58% of Ni, 19% Cr, 13% Co and other additives like Mo, Ti and Al. It shows magnificent strength properties, it can sustain up to 980ºC (1800ºF). It has good corrosion resistance and its resistance to oxidation helps the material to provide service in extreme environment. In gas turbine engine it can withstand temperature of 870 ºC and shows a very good creep rupture strength because of its superiority as compare to alloy 718. Some of its main applications include gas turbine blades, rings, shafts, turbine disk and seals. It is very useful in X-ray fluorescence spectroscopy.

1.3 Application of superalloy in aerospace engine

Superalloys are otherwise very high performance alloy which are very famous for their dynamic purpose. There characteristics like excellent mechanical strength, thermal creep deformation and also possess good surface stability. They also provide resistance to corrosion and oxidation. It has a face centered cubic (FCC) structure which shows austenitic thermal properties. Some of the prominent examples of this type of high performance superalloy are Hastealloy, Incoloy, Waspalloy, Rene, TMS alloy and CMSX single crystal alloys. These super alloys have been derived from both chemical and process inovations. They gain their strength from "precipitation strengthening mechanism". In this strengthening mechanism the secondary phase like gamma prime (γ') and carbide is the form of precipitation. It offers good resistance to corrosion and oxidation due to the presence of elements like Al and Cr. Therefore they are widely used in the manufacture of turbine engine of both aerospace and marine.

1.4 Phases of Ni-based superalloys

Gamma (γ): The matrix of Ni-based super alloy is the main composition of this phase. As discussed above it is the FCC austenitic face in a solid solution**.** The various alloying elements that constitute Ni-based super alloys are C, Cr, Mo, W, Nb, Fe, Ti, Al, V and Ta.

Gamma prime (γ'): The precipitate form is the main constituent of this phase which strengthens the alloy. This phase mainly occurs in inter metallic state of Ni3(Ti,Al) which has a ordered FCC structure. This phase has a lattice parameter which mainly varies approximately by 0.5% Ni(Ti,Al) and Ni atoms are present at the cube phases or at the cube edges. As the γ' precipitation is aggregated, the energy decreases in the direction <1 0 0> forming cuboidal structure. So these phase mainly used to improve strength of super alloy.

Gamma double prime (γ"): This phase particularly consist of Ni3Nb or Ni3V and is used to increase the strength of Ni-based superalloy even at low temperature i.e. (<650ºC) as compared to γ'. It is a body centered trigonal (BCT) structure and in the direction of <0 0 1> planes which is //ly aligned to the γ family. The phase precipitate as 60nm by 10nm discs. Due to which there is a lattice mismatch between the BCC and FCC structure. This may lead to increase in the strain value together with order hardening which is the main reason to increase the strength of component. When the temperature goes beyond 650ºC, then γ" is generally unstable.

Carbide Phases: These phases are generally stable, they prevent deformation at high temperature. Carbide forms present at the grain boundaries.

Topologically closed pack (TCP) Phases: This phase is a combination of family of phases like sigma (σ) phase, X phase and μ phase. These are actually not closed pack but due to brittleness and depletion of γ matrix are used to characterize at TCP phase. These phases can be seen when the temperature goes beyond 750ºC.

1.5 Micro-structure of Ni-based superalloy

Al atoms are present at each vertex of cubic cell in the form of sub lattice 'A' in case of pure Ni3Al phases whereas atom of Ni phase present at phase centre and form sub lattice 'B'. It is a non-stoichiometric structure because one can find lot of vacancies or voids in the sub lattice which makes stoichiometric imperfect. Sub lattices A and B when present in γ' phase can dissolve a good number of element. For the selection of blades in a gas turbine engine Nimonic series alloy are mainly used. These alloy form precipitation in a γ matrix at the grain boundaries for increasing the strength of grain boundaries. Al, Ti, Ta and Nb are particularly known as the 1st generation super alloy. Example of 1st generation super alloy is Rene N4 in which the fractional volume is about 50 to 70% of γ' precipitations. Rhenium which is a 2nd generation superalloy some time acts as a slow diffuser and separates from the γ matrix. There by decreasing the rate of diffusion but it improves the service temperature by 60ºC. There are certain advanced coating techniques being used to counteract the loss of oxidation resistance by diffusing the Cr content. Example of 2nd generation includes Rene N5 and CMSX 4. Other 3rd generation alloys are CMSX 10 and Rene N6. Ruthenium is a 4th generation super alloy which is being developed and which is very expensive. Now-a-days there has been widely application of single crystal super alloy because of their unidirectional solidification technique. There is no grain boundary formation because many mechanical properties is very much dependent in the formation of grain boundaries.

1.6 Incoloy 825

It is a combination of Cu and Mo alloyed together in requisite proportion. It provides significant resistance to many external corrosive environmental factors. It is same as as Incoloy alloy-800 but its resistance factor is bit on higher side on aqueous corrosion which shows resistance for both oxidizing and reducing agents like sulphuric and phosphoric acid. It has its applications in industries like pollution controlled equipment, nuclear fuel

reprocessing, chemical processing, acid production etc. The Incoloy 825 available in market generally appeared in the form of sheet, pipe and tube (welded and seamless). There are certain characteristics like Incoloy 825 a given below i.e.

- Enough resistance for the localized attack like oxidation and reduction phenomena.
- Satisfactory resistance to stress corrosion cracking.
- Excellent resistant to pitting and crevice corrosion at room temperature and at elevated temperature of 1000ºF. It shows very good mechanical properties.
- It permits manufacturing of pressure at wall temperature subjected to 800 ºF.

At the time of cryogenic operation it should be operated at high temperature in order to get good mechanical properties. There will be immediate effect of microstructure change at the temperature above 1000 ºF. And it has impact strength and low ductility. We can't use Incoloy 825 when creep rupture properties are the key factor in determining the design properties. Because of the addition of metal like Mo, Cu and Ti, it shows exceptional resistance towards excessive corrosion environment. The austenitic structure in Incoloy 825 is quite stable because of high Ni content, it is sufficient enough to resist stress corrosion cracking. Due to intergranular attack in this alloy, Ti acts as a stabilizing agent. Sulphuric and phosphoric acid plays an important role in offering resistance to corrosion. The availability of Incoloy 825 in the market is in the form of sheet, plate, rod, wire, tube, pipe etc.

1.7 Applications of Incoloy 825

- Phosphoric and sulphuric acid evaporators and vessels.
- Acid pickling, tank and heaters.
- Design of propeller shaft and tank trucks.
- Power station ash hoppers.
- Hot vessels for food, water and sea water.

1.8 Micro machining

It is the process of removal of very less quantity of material (particularly metal) by implementing processes like drilling, planning and shaping instead of using very sharp edge tool is defined as micro machining. In other words it also defined as process of super finishing a material by producing very fine surface finish. The need of micro machining

arises mainly due to the demand in the production of miniaturized devices in the range of very few hundred microns which are become very useful in the field of electronics, medicine, bio-technology and communications etc. Due to the rising demand a variety of micro machining technique like deep reactive ion etching, electrical discharge machining, laser machining and CNC are implemented now-a-days. In the process of micro machining the tools used for drilling or turning is very smaller in size in the range of 10µm in diameter. Micro machining is very useful in end mills where the diameter of variation is very small and lies in the range of 100 to 500µm. In ancient time the parts of a wrist watch where the only micro products manufactures but now-a-days due to the heavy demand of more number of micro parts in various industrial products has given micro machining a certain priority. Electronics circuits have devices with micro dimensions present on the printed circuit board. Also it is useful in the fuel injection nozzles for automobiles because of severe environmental problem, noising due to pollution has lead in the design of very smaller nozzle with much more accuracy. Therefore micro machining is a very crucial technology that fulfils all the above requirements for manufacturing of micro products. Micro machining in other words is a synonyms of micro processing.

1.9 Classification of micro machining

Micro machining process classified as shown in below Fig1.1 i.e. it is basically divided into two different parts that is conventional and non-conventional micro machining whereas micro drilling and micro milling process undergoes conventional machining. Non-conventional machining classified into three different ways i.e. mechanical, beam energy based and chemical & electro chemical micro machining process. Mechanical micro machining processes include USMM (Ultrasonic micro machining), AJMM (Abrasive jet micro machining), AWJMM (Abrasive water jet micro machining), and WJMM (Water jet micro machining). Thermal micro machining processes include EBMM (Electron beam micro machining), IBMM (Ion beam micro machining), and PBMM (Plasma beam micro machining). Chemical and electro chemical micro machining processes include PCMM (Photo chemical micro machining) and ECMM (Electro chemical micro machining).

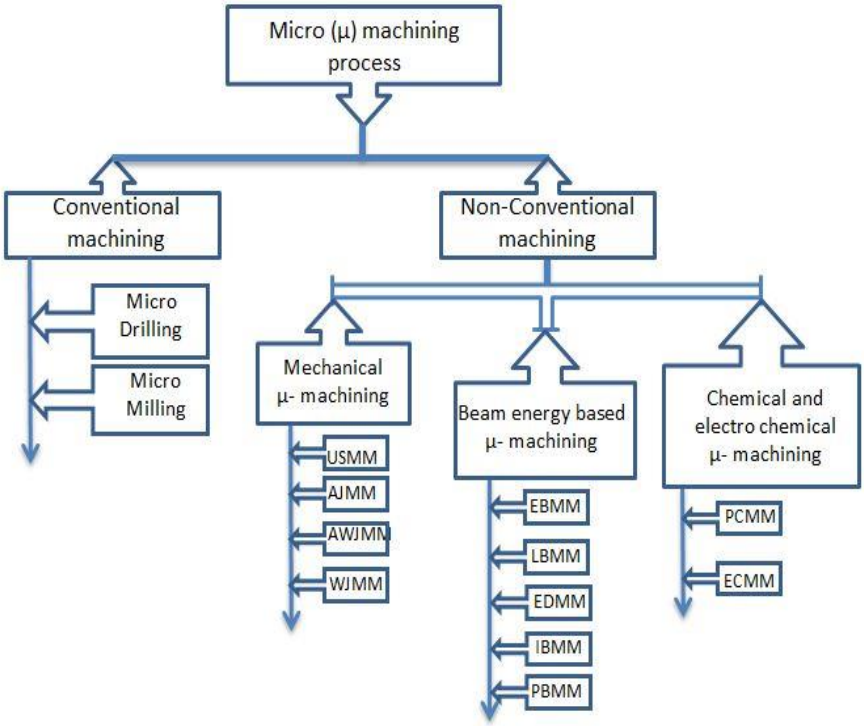

Fig.1.1 Classification of micro machining

1.10 Micro drilling

Micro drilling is a method of proper rotation of micro drill which produces smooth surfaces by conventional process. Generally it is a process in which in micron level metal will be removed and having drill diameter of less than 500μm. Micro drills don't have helical flutes which has generally available in conventional drills. Micro drills generally made up of micro grains, tungsten carbide or cobalt steel. These are less expensive but quick to grind and lack in strength as compare to the tungsten carbide drills. The point angle in these types of drills depends upon the material to be drilled. The general point angle lies between 118º to 135º while drilling hard materials. The drill is mounted on the mandrel and the mandrel axis never coincides with the workpiece axis. So a proper offset value is provided in order to avoid vibration. When a drill is continuously withdrawn and again inserted in the hole to be drilled, at that time peck cycle of micro drill is considered. It helps in cleaning chip present inside the hole. The normal speed and feed recommended for micro drilling is changed according to the material to be drilled. But there is a disadvantage of micro drilling because of drill geometry. Therefore they have a L/D ratio of 4 to 14. Fig.1.2. shows an arrangement of micro drilling set up i.e. a mechanical micro drilling arrangement, in which spindle is controlled by computerized program and

dynamometer connected with charge amplifier. When drilling operation carried out forces are measured by data acquisition system and machining operation done. In general micro drilling process can be carried out by non-traditional machining process like micro ultrasonic drilling, micro laser beam drilling, micro water jet drilling, micro electrical discharge machining, micro electro chemical machining etc.

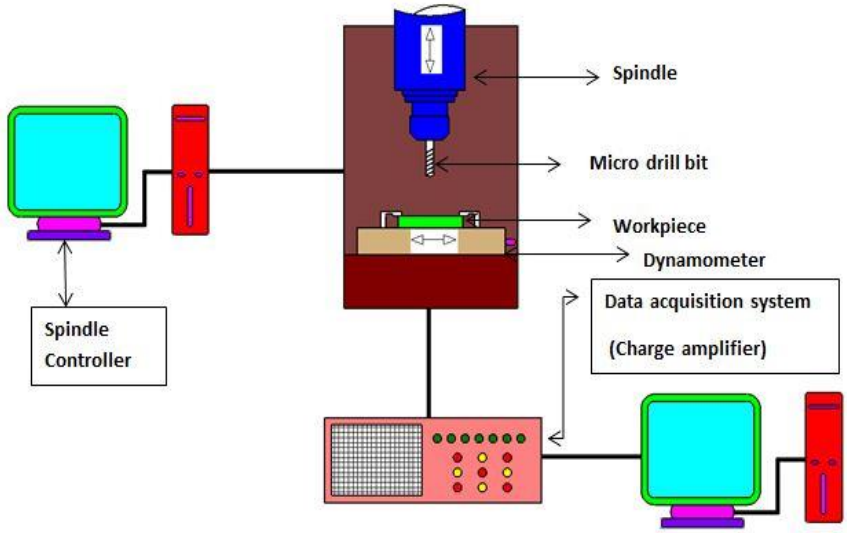

Fig.1.2: Micro drilling set up arrangement

In many aspects there is no difference between micro and macro drillings but fundamentally they are different in size, cutting mechanism, ratio of uncut chip thickness to edge radius etc. In micro machining to get minimum chip thickness, the depth of cut needs to be larger than the critical chip thickness formed due to the elastic effect. The relationship between the tool radius and minimum chip thickness depends on the cutting edge radius and the material of the workpiece. Out of all the problematic issues, the measurement of forces is extremely challenging due to the size of tools and small values of the forces. If noise present then it disturbs the signal and gives distorted results. Applying merchant's cutting model that is used for macro cutting processes is not useful for micro machining. This is due to the effects of edge radius, which results in high negative rake angles and elastoplastic effects. Presence of high negative rake angles also affects the magnitude of shearing and plowing, resulting in a substantial increase in the axial force and increased friction on the rake face of the tool. The shearing and plowing effects would result in the need for a relatively large volume of material to become fully plastic for a relatively small amount of material to be removed, which would cause

significant increase in the specific energy. Beside this the relationship between the tool radius and minimum chip thickness depends on the cutting edge radius and the material of the workpiece.

1.11 Applications of micro drilling:

- Cooling channels in turbine blades
- Printed circuit boards in electronic products
- Micro electromechanical systems
- Fiber optic products
- Flow measuring devices
- Fuel injection nozzles

CHAPTER 2

Literature Review

2.1 Effect of machining parameters on micro drilling

Micro machining operated components which are generally made up of composites are very common in aerospace and automobile industries. Rahamathullah and Shunmugam [1] have used carbide drill bit of 0.3mm diameter for micro drilling of GFRP. Apart from parameter like speed and feed rate, the research mainly focused on high quality hole with efficient drill life. There experiment conducted on blind hole drilling, resulted the maximum thrust force and reduction of torque. They have also done, through hole drilling at peck cycle for different fibre reinforced specimen to determine the regression models which showed good result with the theoretical one. The experiment purely based on producing holes having large aspect ratio by choosing proper drilling parameters. Under various cutting condition Imran et. al [4] studied the mechanism of micro drilling. There experiment is based on feasibility of Ni-based super alloy used in deep hole micro drilling. This resulted in obtaining holes of high quality and good surface integrity. Their research work is mainly focused on geometry of producing hole in Ni-based super alloy. This helped them in choosing commercial micro drills within selected ranges for carrying different operations. They formulated different strategies ensuring continuous loading of pilot drills by reducing the chances of breakage in drills. There results reveal fine hole micro drilling of Ni-based super alloy. By applications of DOE method Woo Kim et. al [6] attempt to reduce the thrust forces in step feed micro drilling process. Optimization carried out by combining the drilling thrust, three cutting parameters, feed rate, step feed and cutting speed. Orthogonal array L27(313) is generated and ANOVA (Analysis of Variance) is calculated for experimental analysis. Finally Woo Kim et. al [6] concluded that feed rate is the most important factor to reduce the micro drilling thrust force. Zheng et. al [7] carried out the micro drilling experiment by using PCB board as a workpiece with 0.1mm diameter drill bit at rotational speeds of up to 300 krpm. Under digitally photo graphed the whole process analyzed and influence of cutting conditions on drilling process and hole quality were observed. They found that the morphology of the chips and the hole wall surface depended on the material properties of the printed circuit board. Chip morphology affected by feed rate, spindle speed and tool wear as well as hole quality

affected. The basic mechanism of micron material removal of PCB board analyzed. Lianq Chern and Jou Lee [10] investigated that the effects of assisted vibration on the drilling quality of aluminium alloy (Al 6061-T6) and structure steel (SS41) with twist drill size of 0.5mm. They have taken a new approach to obtain the desired vibration was proposed from the workpiece side, by a self-made, vibrating worktable. They found that hole oversize, displacement of the hole center, and surface roughness of the drilled wall could be improved with the increase of vibrating frequency and amplitude. Roundness of the drilled hole could also be improved when high amplitude and proper frequency are imposed. Okasha et. al [12] approached a new feasibility for micro drilling of Inconel 718 alloy sheets at an acute angle by using sequential laser and mechanical drilling. They demonstrate the comparison between both sequential laser and mechanical micro drilling process and analyzed that mechanical micro-drilling produces good quality holes as compare to sequential laser. Mechanical drilling faced problem to drill holes at acute angle. Rahamathullah and Shunmugam [13] attempt to drill micro-holes in carbon fabric laminate composites using 320 µm diameter carbide drills. They conducted the micro drilling experiment according to full factorial design. During machining thrust force and torque were measured and by using these values regression model developed. There result indicated that by selecting proper process parameters, the good quality of micro holes could produce and also delamination damage, roundness error and diameter of these drilled holes were measured and analyzed with variation of the process parameters. Patra et. al [15] investigated on micro drilling of austenitic stainless steel as workpiece and 0.5mm diameter solid carbide micro drill bit. Full-factorial design of experiment were performed by taking two factors i.e. speed and feed and three level i.e. low, medium and high. For developing mathematical model for cutting forces in micro drilling RSM (Response surface methodology) was used. Experimentally they analyzed that feed affected the cutting force components (radial and thrust) significantly. Additionally, it also showed that there were only minor effects from cutting speed, square of cutting speed, square of feed and product of speed, and feed on the cutting forces. They finalized that the optimized cutting conditions were proposed for minimum cutting forces. Abdul Rahman et. al [16] presented the effect of drilling parameter such as spindle speed, feed rate and drilling tool size on material removal rate (MRR), surface roughness, dimensional accuracy and burr. They studied on optimum drilling parameter for HSS drilling tool in micro-drilling processes in order to found the best drilling parameter for brass as a workpiece material and 0.5 mm to 1.0 mm drill sizes were performed by changing the

spindle speed and feed at three different levels. They analyzed that the spindle and feed rate increased then the surface roughness decreased. The value of MRR decreased when the tool diameter, spindle speed and feed rate were decreased. Whereas drilling tool diameter, feed rate and spindle speed increased then the dimensional accuracy of drilled hole decreased. The increment of spindle speed and feed rate value mostly affected the tool wear and size of burr on the edge of drilled holes. Watanabe et. al [18] done the experiment on micro drilling by taking Printed circuit board as workpiece and micro drills of 0.1mm diameter at a rotational speed of 3×105 min−1. They focused on radial run-out and carried out the correlation between the radial run-out of drills and the hole quality. They concluded that after contacting the drill bit with the work surface, the drills which revolved orbitally with the radial run-out, moved toward the centripetal direction. Because of the centripetal action the hole quality is intensive to drill wear as well as hole quality. Huang et. al [21] developed one image processing technique in which easily defects in micro drilling detected during machining which is very much helpful to study the effect of micro drilling. HORIUCHI et. al [22] analyzed that during micro drilling due to increase in the rigidity of drill beam, the radial force increased as the depth of hole increased.

2.2 Effect of environment on micro drilling

Soo Nam et.al [2] have developed drilling machine tool for carrying out number of experiment in case of compressed air lubrication, pure MQL and nano fluid MQL. In this paper experimental method is carried out for micro drilling operation using nano fluid MQL, pure MQL and compressed air lubrication. The diameter of 30nm is used in the nano fluid MQL with based fluid of paraffin and vegetable oils. Holes of diameter 200µm were drilled using uncoated carbide twist drill bit in Al6061 workpiece. There experiment shows tremendous increase in the holes drill there by reducing the torque and thrust force. Whan Kim et. al [3] are studied drills with unstable drilling process which produces insufficient cutting fluid supply with an increase in the depth of machining. It leads to the serious problem issue in micro drilling operation. There experiment is based on peck drilling of 1 step feed length as compare to the drill diameter. The range of 1 step feed length is always chosen to be random. These parameter is used in monitoring for peck drilling are induced by considering thrust force in time as well as frequency domain. There monitoring was based on a software called ‘Lab View’. By using this, a stable drilling condition was obtained for drilling of steel and Al. Imran et. al [8] focused on mechanical drilling of micro drills under wet cutting conditions by taking Inconel 718 as

workpiece. They revealed three different zones i.e. a highly deformed nanostructured surface layer containing ultrafine and high aspect ratio grains drawn out by large scale deformation, a deformed subsurface layer and finally the unaffected parent metal. The nano-hardness, plastic deformation, microstructure and crystal misorientation were observed. The correlation between the modified surface and subsurface layers and the cutting conditions was established by them. The phenomena behind the formation of the different zones were investigated. They suggested that subsurface alterations were driven by thermo-mechanical loading, causing plasticity and grain refinement by excessive shearing local to the cut surface. Biermann et. al [19] analyzed the chip formation while making a small diameter deep hole drilling on difficult-to-cut materials under minimum quantity lubrication. They used difficult-to-cut material like Ni-based super alloy Inconel 718 and the the bainitic steel 20MnCrMo7. Ucun et. al [20] investigated the effect of coating material on tool wear of milling of Inconel 718 in micron conditions. Under dry and lubricated condition experiment was carried out. They concluded that due to lubrication, the edge radius of cutting tool reduced due to decreased in cutting force.

2.3 Effect on Surface Integrity during micro drilling

The surface integrity and wear mechanism is the main aspect used in this paper for micro drilling of Inconel 718, Ni-based super alloy under both dry and wet condition. The metallurgical behavior of the material studied by using machines like SEM, BSEM and TEM. Due to the formation of large scale in surface deformation along with a dislocation density which is very high to determine the surface integrity of nano crystalline structure. The depth of affected layer, the micro structure and energy stored within it are determining the cutting condition taken initially. The wear mechanism under wet cutting are micro chipping, abrasion and diffusion whereas for dry cutting the mechanism listed are high adhesion and catastrophic failure. The result thus obtained helps in determining the cutting fluids taken for getting better surface integrity. Nakagawa et. al [17] indicated the appropriate method to improve the drilled hole wall quality by making micro drill on printed circuit boards (PCBs) and calculated torque values, temperature and surface roughness of drilled holes. They concluded that the surface roughness of hole wall increased with temperature of drill. And the drill temperature increased due to friction between hole wall and the land or margin of drill. For which to obtain high quality micro-drilled hole wall basically the reduction of the workload by the friction seemed to be effective. Thakur et. al [23] studied that during dry turning the effect of cutting speed and

CVD multilayer coated tool on machined surface of Inconel 825. They observed that after machining, in case of both coated and uncoated tool the white layer thickness increased with increased in cutting speed. Again Thakur et. al [24] investigated that during dry turning uncoated tool performed poor surface finish than coated tool only at higher cutting speed. Various macro features came to know that white layer thickness and grain refinement increased with increased in cutting speed. As compared to uncoated tool with coated tool, at low and medium cutting speed white layer formation prevented and work hardening tendency of Inconel 825 decreased.

2.4 Modeling and simulation

Hinds and Treanor [9] analyzed stresses in micro drills by using finite element method. They have taken the workpiece as printed circuit board and 0.1mm diameter of drill bit with restricted operating parameters. By setting node points of the drill geometry the three dimensional models of drills were defined. Drill loading determined from FEM by using force value which measured from experimental tests. They presented principal stress isograms on drill cross-sections for different drill geometries and correlated with actual drill life. Shi et. al [11] purposed to obtain the micro drill bit temperature field distribution in micro-drilling process and the temperature drop in retracting process with simulation software. They found that high temperature focused in the cutting edge and chisel edge, high temperature of micro drill bit increased with increase of spindle speed and feed. There invented temperature measurement method could satisfy most of the requirements of temperature measurements. Sahoo et. al [14] indicated that stresses plays an important role for influencing hole quality. Hole diameter reduced due to increase in feed rate whereas delamination factor and mean bur thickness increased. They utilized finite element analysis (FEM)-based simulation of deformation and equivalent stresses to explain various characteristics of micro hole which is obtained from surface integrity study.

2.5 Motivation and objectives

From the review of past literature concerning micro machining, it has been found that extensive studies have been under taken on PCB which is a composite material. Similar studies on metallic alloys, Ni-based superalloys in particular, are comparatively fewer. Only one research group has studied micro drilling of Inconel 718. Similar endeavor is also read in micro drilling of other grades of Ni-alloys. Although modelling of micro

drilling process has been carried out, the same also needs to be correlated in to different characterization in micro drilling. Surface integrity in micro machining is one of the critical issues that affect the performance of process. As such, literature on surface integrity is scarce and needs much more research attention.

Keeping in view of the in completionism in the previous studies, the objectives of the present research work are specified below.

1. To investigate the effect of spindle speed and feed on thrust force, radial forces and torque in the machining of Incoloy 825, a Ni-based superalloy.

2. To carry out FE modeling of deformation and equivalent stress at various section of the micro drill under different condition of cutting speed and feed.

3. To study the effect of spindle speed and feed on surface roughness and oversize error of micro holes.

4. To investigate the influence of the same cutting parameters on the formation of circumferential deformation layer, white layer, plastic deformation of grains at the sub surface regions.

5. Statistical analysis of experimental data and development of predicted models.

CHAPTER 3

Experimental Details

In this chapter detail methodology of the experiment has been described. The detail aspect of machine tool used, equipment facilities, workpiece material, cutting tool, machining parameters and experimental set-up has been discussed.

3.1 Details of cutting tool

Carbide uncoated drill bit with specifications conforming to SD26-0.40-2.70-3R1 was used as the tool material. The tool geometry can be described as:

Table.3.1: Detail features of tool geometry

Diameter of Drill Bit	0.4 mm
Major cutting edge angle	65˚
Point angle	130˚
Flute length	3.6 mm
Total length of insert	38 mm
Shank diameter	3.0 mm
Shank type	Cylindrical
Grade	Carbide uncoated

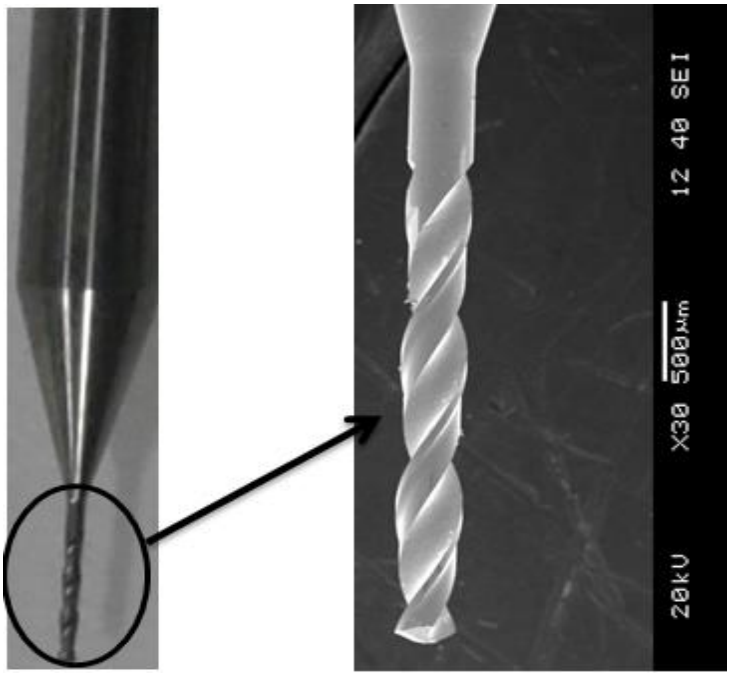

Fig. 3.1: Carbide uncoated drill bit

3.2 Workpiece Description

Micro drilling operation carried out on Ni-based superalloy Incoloy 825. A circular sample of Incoloy 825 was taken with a diameter of 35mm and thickness of 3mm. The sample was cut from the parent stock with the help of wire-cut EDM machine and polished the surface by using different grade of sand papers to get a polished surface for micro drilling. The chemical composition and properties of Incoloy 825 in detail is described below:

Table.3.2: Chemical composition of Incoloy 825

Elements	**Ni**	**Fe**	**Cr**	**Mo**	**Cu**	**Ti**	**C**	**Mn**	**S**	**Si**	**Al**
% by mass	38.0-46.0	22	19.5-23.5	2.5-3.5	1.5-3.0	0.6-1.2	0.05	1.0	0.03	0.5	0.2

Table.3.3: Physical and mechanical properties of Incoloy 825

Density	8.14 (kg/m^3)
Specific Heat	440 (J/kg. ˚C)
Melting Range	1350 – 1400 (˚C)
Tensile strength	772 (MPa)
Yield Strength	441 (MPa)
Young's Modulus	196 (GPa)
Poisson's Ratio	0.29

3.3 Selection of Cutting Parameters

Owing to low thermal diffusivity and strain hardening tendency, elevation of cutting speed and feed has always been challenging in the machining of Ni-based super alloys. According to a good number of studies [2, 5] recommended range of cutting speed is 10 to 40 m/min while using cemented carbide tools. However during micro drilling of Incoloy 718, still lower range [4] was employed to avoid drill breakage. During trial experiments of the current study, drill breakage was not observed up to a spindle speed of 30000 rpm. It has been, therefore, decided that to accept the general recommended range for Ni-based superalloy. There spindle speeds of 10000, 20000 and 30000 rpm were accordingly selected and the corresponding cutting speeds were 12.56, 25.12 and 37.68 m/min respectively.

Feed (f) is a very important parameter in micro drilling, since it influences chip load which intern dictates cutting mechanics and hence machining performance. To be more precise the ratio of undeformed chip thickness i.e. chip load and edge radius (r), in other words f/r, has major impact on forces, torque, tool wear and surface integrity. In traditional (macro) drilling, higher feed and edge radius are employed. However during downsizing the drill, so as to use in micro drilling operation reduction in edge radius to the equal proportion of undeformed chip thickness is practically challenging task. This is due to the requirement of ultra precision during grinding cutting edge. In the work of Imran et.al [4, 5, 8], drill bit of 2µm edge radius was used, the current study is owing to lack of pertinent technical data from the catalogue of the tool manufacturer combined with considerable difficulty in sectioning the cutting edge of the micro drill, exact value of r is unknown and hence similar value close to 2µm is assumed for selection of feed. Accordingly, four different values of feed i.e. 1, 4 8 and 12 µm/rev where finalized for the present investigation. Lower feed other 1 µm/rev might lead to a great deal of rubbing and ploughing due to edge rounding higher than undeformed chip thickness. On the other hand, high feed rate that 12 µm/rev might increase cutting force deformation and temperature to an unacceptable range.The machining operation was carried out under variable speeds of 10000, 20000 and 30000 rpm for the feed rates of 1, 4, 8 and 12 µm/rev and at constant depth of 1.25 mm in flood environment i.e. with use of coolant or cutting fluid named HOCUT795H (with 10% concentration has been used for lubricated machining).

Table.3.4: Cutting Parameters

Speeds (rpm)	10000, 20000, 30000
Feed rates (µm/rev)	1, 4, 8, 12
Depth of hole (mm)	1.25
Cutting environment	Flood
Type of hole	Blind hole
Method of drilling	Direct drilling
Hole diameter (mm)	0.4

The appropriate process parameters for 12 different holes are shown in the table:

Table.3.5: Conditions for different holes

Hole No.	Speed, rpm	Feed rate, µm/rev
1	10000	1
2	10000	4
3	10000	8
4	10000	12
5	20000	1
6	20000	4
7	20000	8
8	20000	12
9	30000	1
10	30000	4
11	30000	8
12	30000	12

3.4 Machining Performance Evaluation

Machining operation i.e. micro drilling was performed on Ni-based superalloy Incoloy 825 to examine the performance of uncoated drill bits. Since Incoloy 825 comes under the category of 'difficult-to-cut'' material and particularly micro drilling always poses a challenging task, so it was taken as the workpiece to understand its machinability by judging the desired outputs with the help of the cutting tools. Fig.3.2 shows the photographs of machine tool used for micro drilling of Incoloy 825 which is more robust and unique to minimize the vibration.

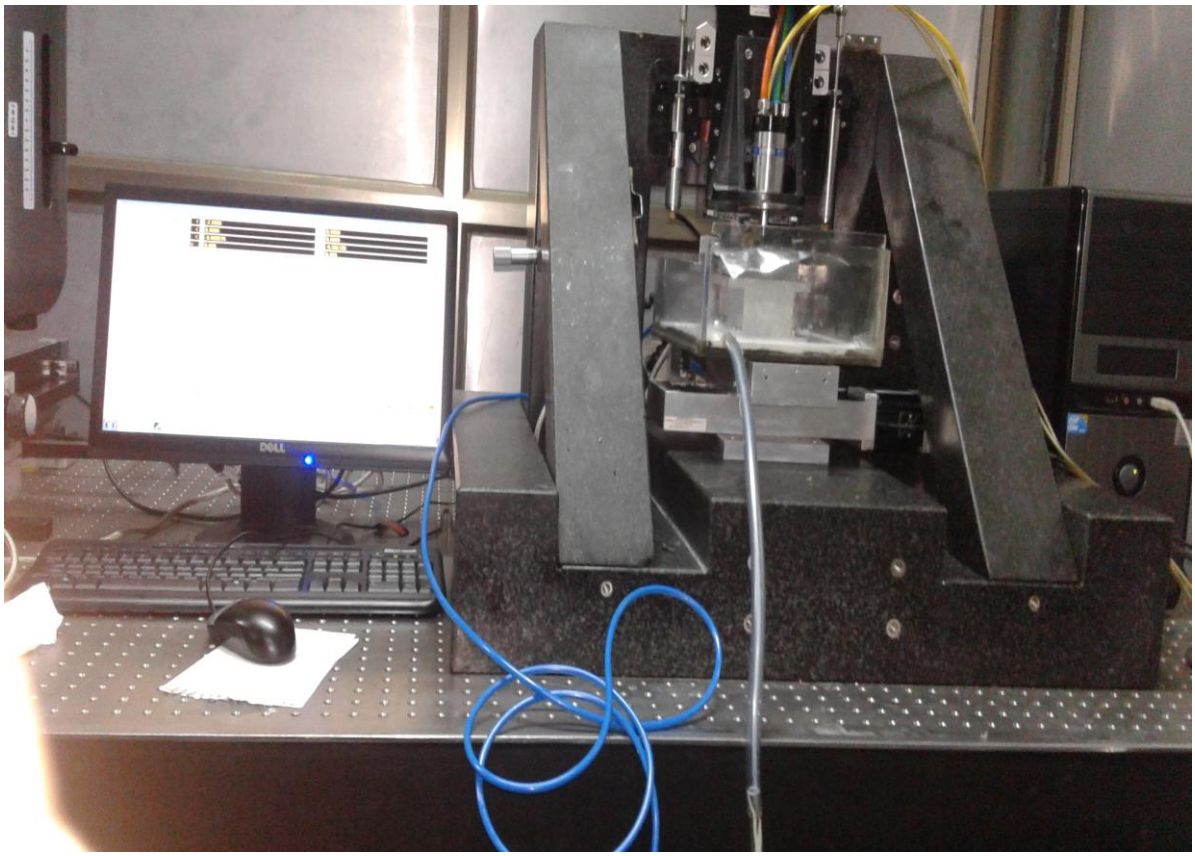

Fig. 3.2: Ultra-high speed micro machine

Table.3.6: Technical description of ultra high speed micro machine

Spindle speed	Up to 170,000 rpm
Maximum Feed rate	0.06-6000 mm/min
Resolution (axes X and Y)	0.5 µm
Resolution (Z axis)	1 nm
Accuracy (axes X and Y)	0.5 µm
Accuracy (Z axis)	0.3 µm
Tool holder	Mega 4S (high accuracy collet with a runout of 1 µm)
Material of base and sideways	Granite

Micro drilling operation was performed at ultra-high speed micro machining centre in machine tool lab, at IIT Bombay (Make: Indian institute of technology Bombay, Mumbai, India;) with positioning accuracy of ± 0.5 µm in X, Y axes and ± 0.3 µm in Z axis. Also having resolution of 0.5 µm in X, Y axes and 1 nm in Z axis. Granite has used to build this precision machine base and sideways because of its low thermal expansion. Granite shows low sensitivity to temperature fluctuations due to its very low thermal conductivity than cast iron. Also vibration absorption is better in granite structures than the cast iron structures. A high speed spindle with a speed range of up to 170000 RPM is mounted on a vertical axis (Z axis) with maximum federate of 0.06 to 6000mm/min. Machining operation was carried out under flood environment and the name of cutting fluid is HOCUT795H (with 10% concentration has been used for lubricated machining), at three levels of speed: 10000rpm,20000rpm and 30000rpm and at four levels of feed: 1µm/rev, 4 µm/rev, 8 µm/rev and 12 µm/rev and depth of cut (1.25 mm). The drill diameter chosen for the experiment was 0.4 mm. The appropriate process parameters for 12 different holes are used.

(a) (b)

Fig. 3.3: (a) Experimental set up (b) Charge amplifier and coolant set up

During the operation a drill tool dynamometer (Make: Kistler; Model: 9256C1) was used to record the forces in X, Y and Z directions. The workpiece is placed on the dynamometer with proper mounting and dynamometer attached with data acquisition system through which we get the force value. Simultaneously spindle attached with the system by proper programming speed and feed rate values were set. And successfully experiment is done without breakage of drill bit.

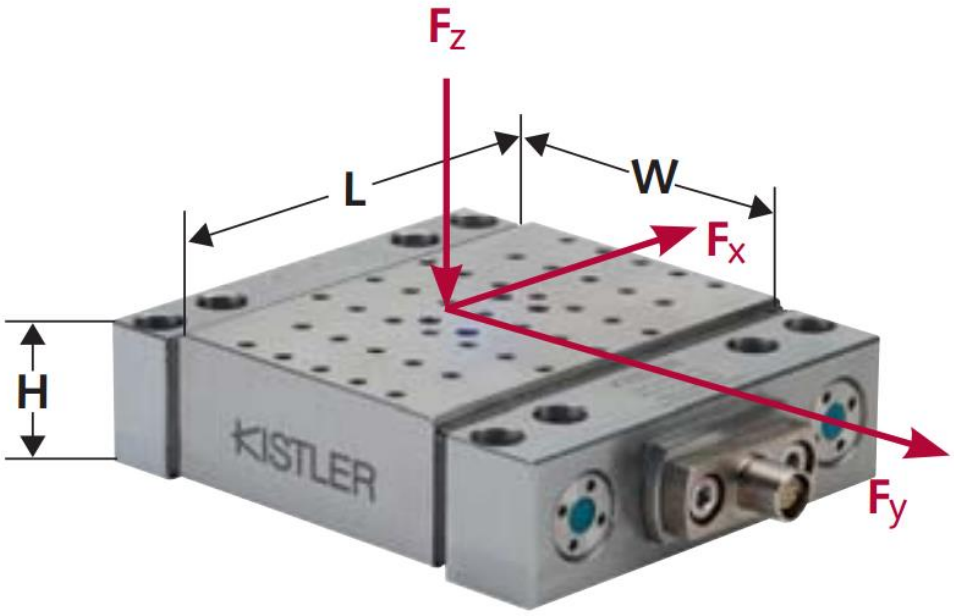

Fig. 3.4: Multi component dynamometer (KISTLER 9256 C1)

Table.3.7: Specification of dynamometer (9256C1)

Measuring range (Fx, Fy, Fz), N	-250 to 250
Sensitivity (Fx, Fz), pC/N	≈–26
Sensitivity (Fy), pC/N	≈–13
Natural frequency, KHz	≈5
Operating temperature range, ºC	0 to 70
LxWxH, mm	80x39x25
Sampling rate	20 KHz

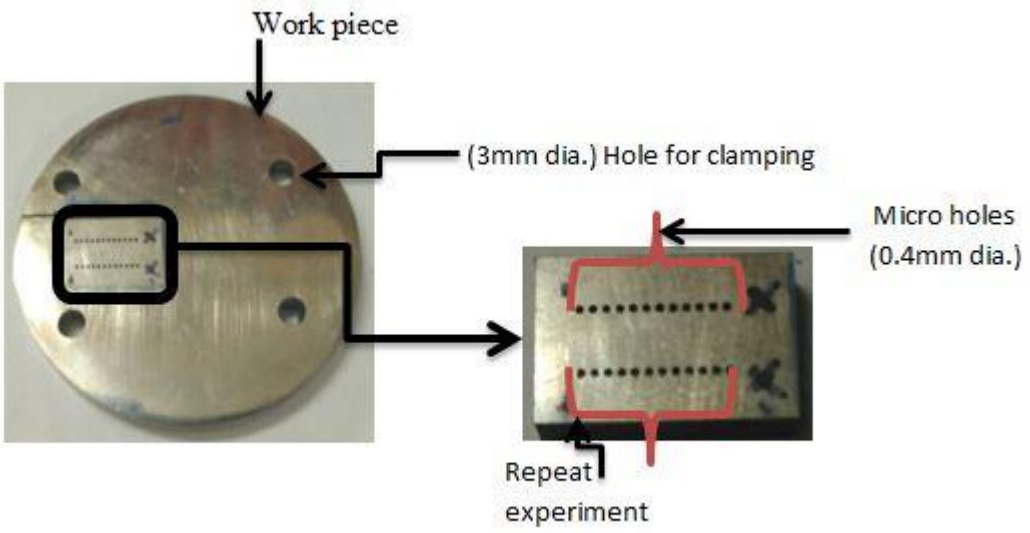

Fig. 3.5: Sample of Incoloy material after micro drilling

After micro machining the state of the workpiece was monitored with the help of profilometer (Make: Zeta Instruments) to determine the surface profile of 12 different hole at different conditions. During measurement the step size is 3.562 µm, the range of focus in Z direction is 1778 µm and with 500 No. of steps, R_a value calculated for each micro hole.

Fig. 3.6: Surface profile measurement setup

After micro drilling operation drilled hole analyzed by using field emission scanning electron microscopy (FESEM) (Make: NOVA NANO SEM-450). Due to high magnification different output responses are localized. Circumferential deformation layer thickness, chip thickness and cracks are shown properly before polishing. After polishing the workpiece with different grades of sand papers and ethching it we found the white layer thickness due to higher magnification.

Fig.3.7: FESEM (field emission scanning electron microscopy)

CHAPTER 4

Results and Discussions

4.1 Experimental Results

Using the experimental data the thrust force (F_z), torque, radial component forces i.e. F_x and F_y were calculated for uncoated tool and the values are tabulated in Table.4.1.

Table 4.1: Experimental forces and torque for micro drilling

Hole No	N, rpm	f, µm/rev	F_z, N	Torque, N-mm	F_x, N	F_y, N
1	10000	1	4.332583	0.00084	0.040522	0.00278
2	10000	4	10.50965	0.00521	0.009287	0.570117
3	10000	8	14.30255	0.01013	0.04025	0.05618
4	10000	12	17.35256	0.01299	0.002534	0.066604
5	20000	1	6.046061	0.00783	0.01958	0.040049
6	20000	4	10.90651	0.00959	0.000382	0.049386
7	20000	8	15.62324	0.01188	0.045264	0.037088
8	20000	12	19.34814	0.01438	0.05829	0.061537
9	30000	1	7.147109	0.01431	0.09968	0.071728
10	30000	4	10.93352	0.01821	0.067616	0.03892
11	30000	8	15.20018	0.02029	0.1213	0.106025
12	30000	12	18.42838	0.2097	0.20931	0.131627

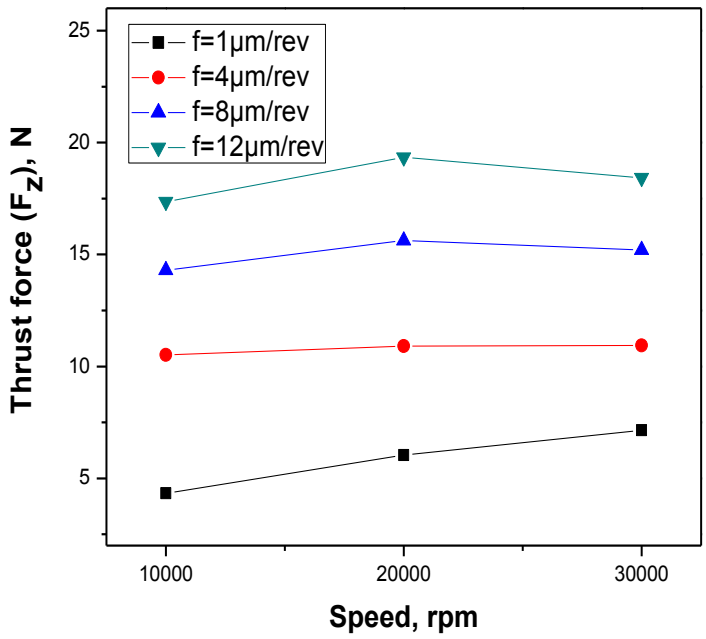

Fig. 4.1: Variation of thrust force (F_z) with speed rpm and feed rate

Fig. 4.1 shows that the variation of thrust force (F_z) with speed rpm and feed rate. There is a clean rise in thrust force with feed due to increase in chip load. Which elevation in spindle speed causes an increase in thrust force under the lowest feed of 1 µm/rev; there was hardly any significant variation in F_z with increase in cutting speed under the condition of high feed. Previous studies on micro drilling exhibited decrease in F_z consistently with rise in cutting speed which was attributed to material softening at high cutting speed. It is interesting to note that two mutually conflicting situations arise with elevation in cutting speed. In addition to thermal softening, deformation induced strain hardening in a typical phenomenon for machining Ni-based superalloy. Therefore these two mechanism tends to balance each other at the feed rates of 4,8 and 12 µm/rev. under hardening due to larger contribution of edge rounding is causing deformation might have led to increasing trend with spindle rpm. Similar trend has been obtained with torque as indicated in Fig. 4.2 Owing to significant fluctuation of torque, maximum peak to valley was considered and demonstrated in Fig.4.2 Such technique has been recommended by Rahamathullah and Shunmugam [1].

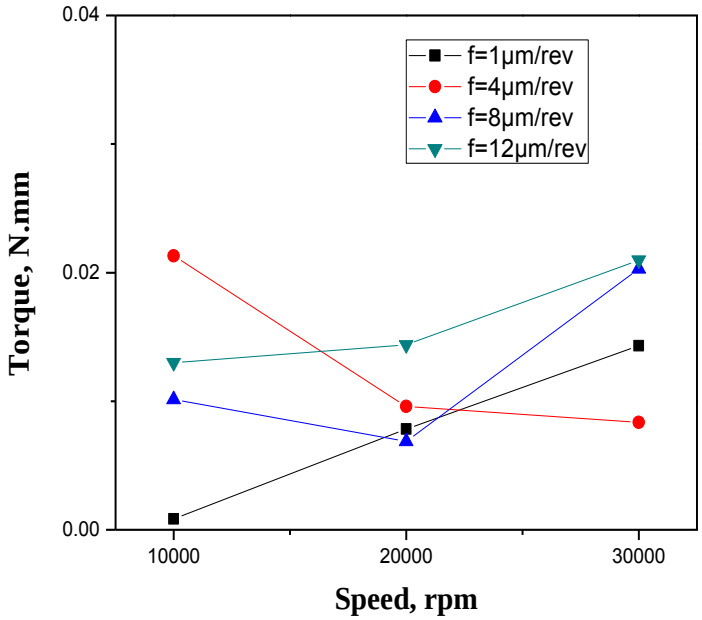

Fig. 4.2: Variation of torque with speed rpm and feed rate

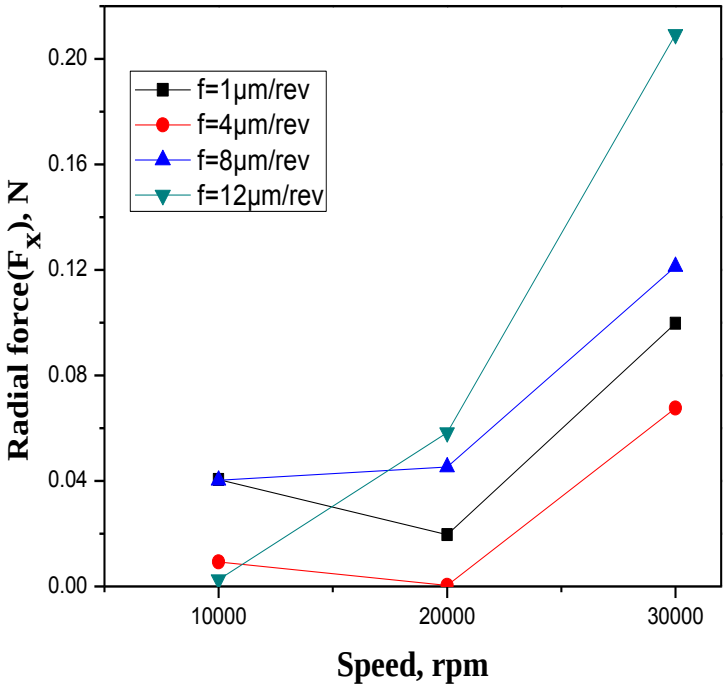

Fig. 4.3: Variation of radial force with speed rpm and feed rate

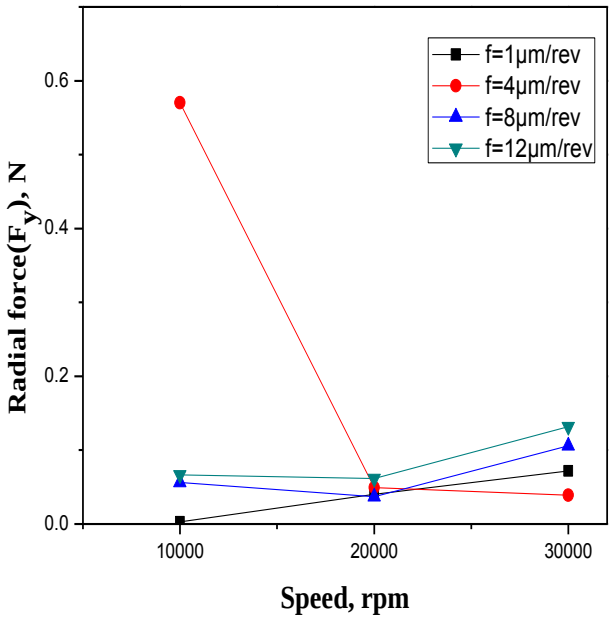

Fig. 4.4: Variation of radial force with speed rpm and feed rate

It is known that radial forces F_x and F_y component does not have much significance on the performance of drilling under macro regime. However, their effect is amplified during micro drilling and they occur due to error in rotational symmetry of the drill lips and margin. These forces are particularly undesirable since they cause wandering of the drill tip at the entrance machining it prone to breakage. These two forces F_x and F_y are plotted in Fig. 4.3 and Fig. 4.4. General trend shows rising trend with cutting speed. Higher value of forces at 1µm/rev compared to 4 µm/rev is again explained by dominance of ploughing effect due to lower undeformed chip thickness than edge radius. It is also to be noted that fluctuation of the signals was higher in case of F_x and F_y, just like torque, compared with F_z. This may be attributed to their sensitiveness to the material inhomogeneity in Ni-alloys owing to presence of hard and abrasive like γ' ($Ni_3(Al,Ti)$). Considering the band width which is produce by plotting the graph between thrust force (F_z) with respect to time. Fig. 4.5 shows the representative image of band width at low speed and high feed rate i.e. (10000rpm, 12µm/rev). Also torque w.r.t time graph plotted and shown in Fig. 4.6 and shows the maximum fluctuation at low speed and high feed i.e. (10000 rpm, 12µm/rev). Fig. 4.6 plotted by smoothing operation for proper analysis.

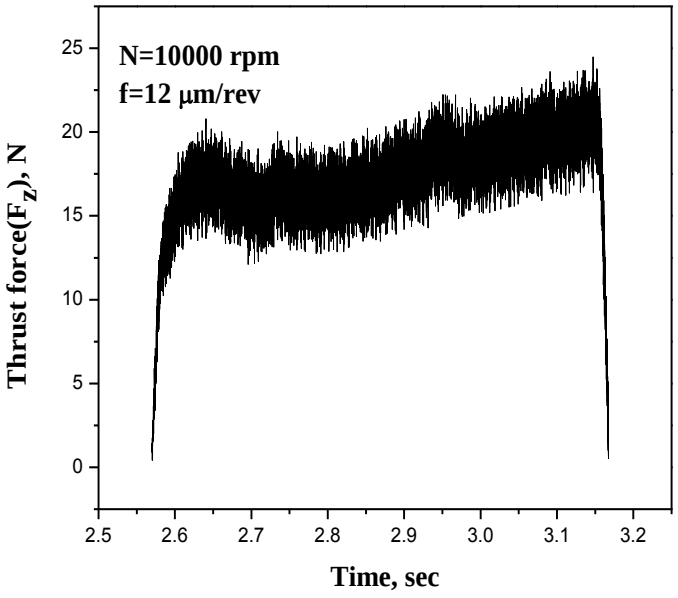

Fig. 4.5: Representative graph of thrust force (F_z) w.r.t time

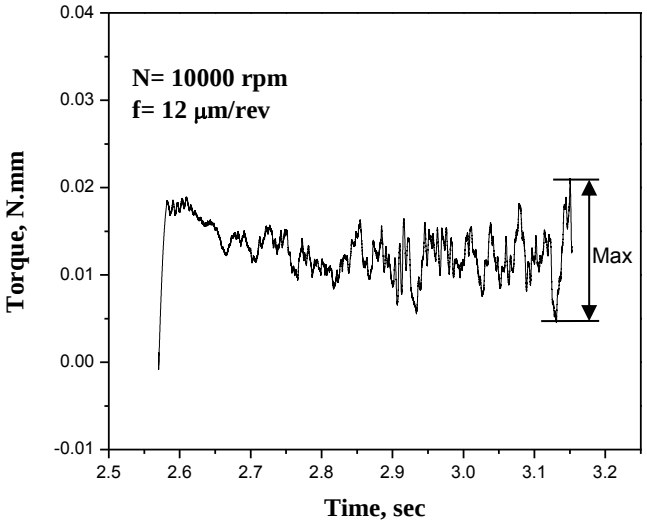

Fig. 4.6: Representative graph of torque w.r.t time

4.2 Simulation

As described in section 3, thrust force (F_z) and torque values obtained through experimentation were utilised in the finite element model for simulation. Deformation and equivalent stress profile were determined and tabulated in Table. 4.2 which also indicates the cutting parameters.

Table.4.2: Simulation data of deformation and equivalent stress generated by micro drilling

Hole No	N, rpm	F, µm/rev	Maximum Deformation, mm	Maximum Equivalent stress, MPa
1	10000	1	0.0059827	180.96
2	10000	4	0.01409	428.35
3	10000	8	0.015962	483.03
4	10000	12	0.019471	589.24
5	20000	1	0.0078472	237.54
6	20000	4	0.01215	367.72
7	20000	8	0.016747	506.68
8	20000	12	0.021394	647.43
9	30000	1	0.0097354	312.47
10	30000	4	0.012407	375.46
11	30000	8	0.017062	516.58
12	30000	12	0.020858	631.38

Fig. 4.10 shows the deformation profile of the micro drill during machining of Incoloy 825. Evidently, primary cutting edge and chisel edge were subjected to maximum deformation in Fig. 4.11. This might be explained by the fact that prior pilot hole was not drilled it led to greater thrust encountered by chisel edge and cutting edge. Slight drifting motion due to very small value of F_x and F_y might also have caused small degree of deformation at the entrance [15]. According to Hinds et. al [9], brittle fracture is the dominant mode of failure for cemented carbide micro drill. Therefore, equivalent stress was simulated and presented in Fig. 4.12. It is again evident that chisel edge experienced maximum equivalent stress under different cutting condition.

A portion of the chisel edge called secondary cutting edge is responsible for material removal and the remaining part tries to indent or push the material ahead. It is now important how these force, torque, deformation and equivalent stress influence different surface integrity characteristics in the micro drilling of Incoloy 825. By using simulated values (which shown in Table.4.2), equivalent stress and deformation plotted with different speed rpm and feed shown in Fig. 4.7 and Fig. 4.8. Stress and deformation are important aspect which can explain various micro drilling performance measures such as enlargement of micro hole, surface roughness, formation of deformation thickness and white layer. The meshing of micro drill bit shown in Fig. 4.9.

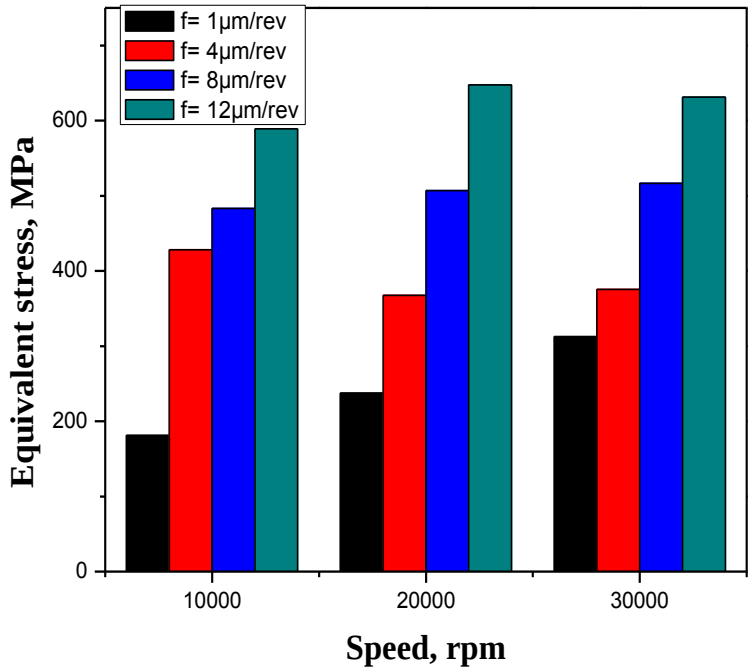

Fig. 4.7: Variation of equivalent stress with speed rpm and feed rate

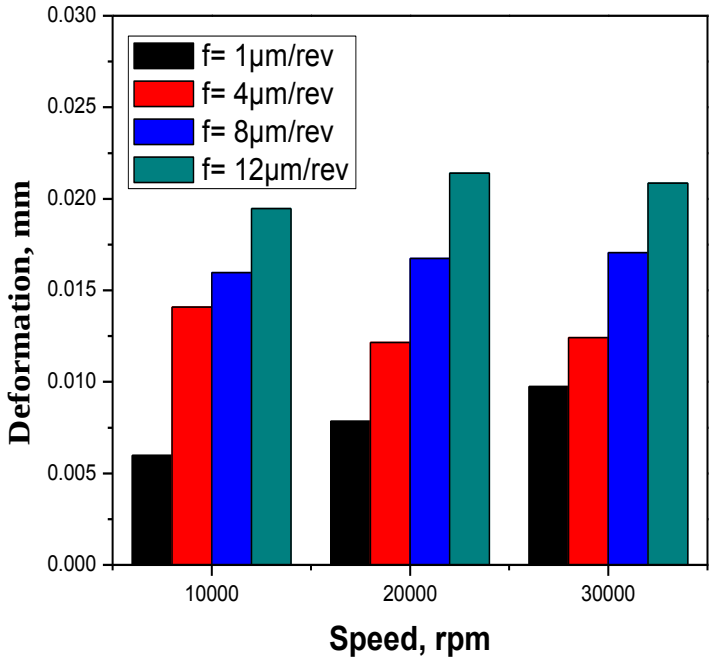

Fig. 4.8: Variation of deformation with speed rpm and feed rate

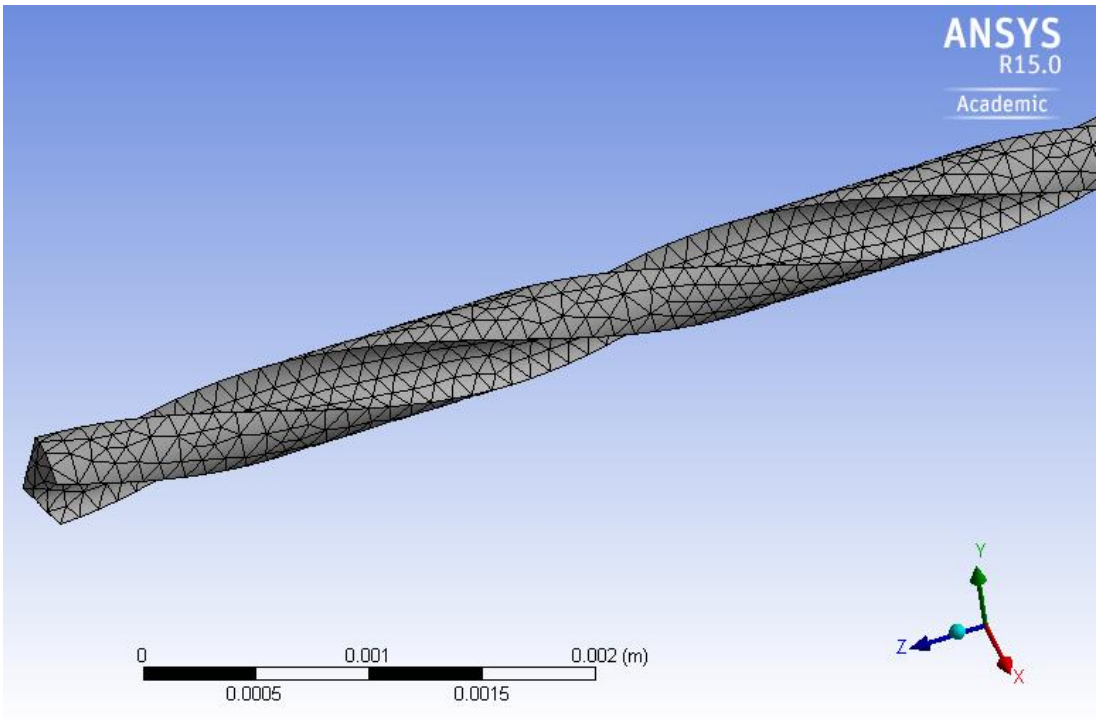

Fig. 4.9: Meshing of micro drill bit

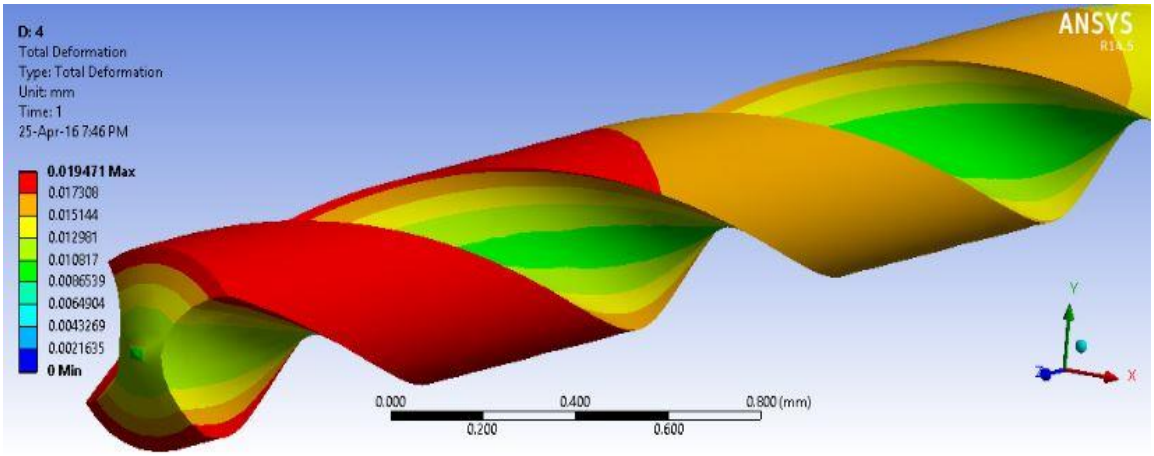

Fig. 4.10: Representative image of deformation at condition (10000 rpm and 12µm/rev)

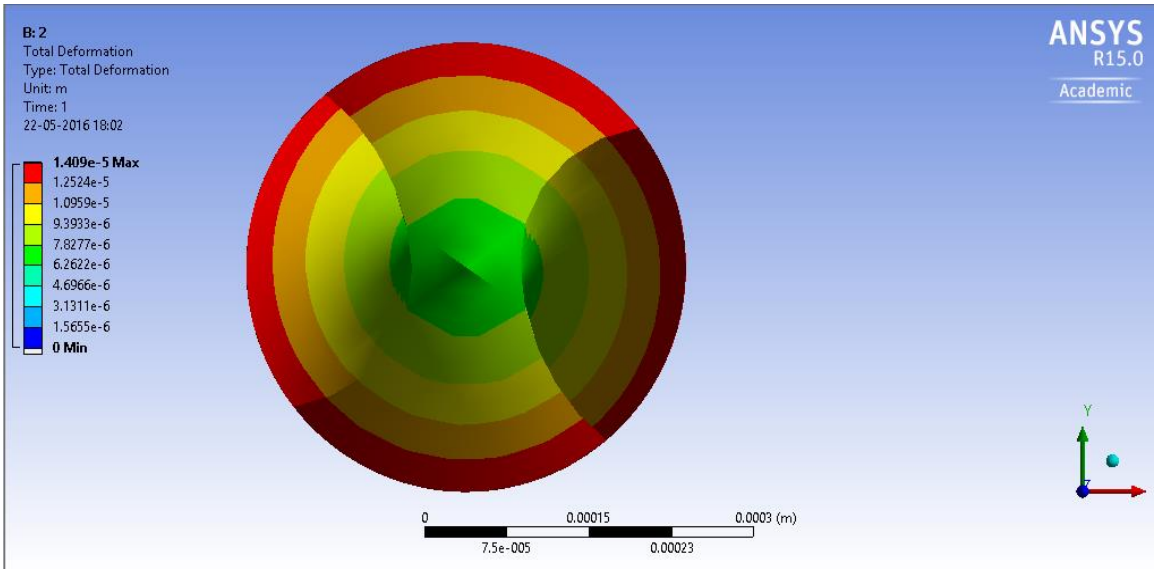

Fig. 4.11: Total deformation in axial and diametric plane at condition (10000 rpm, 12µm/rev)

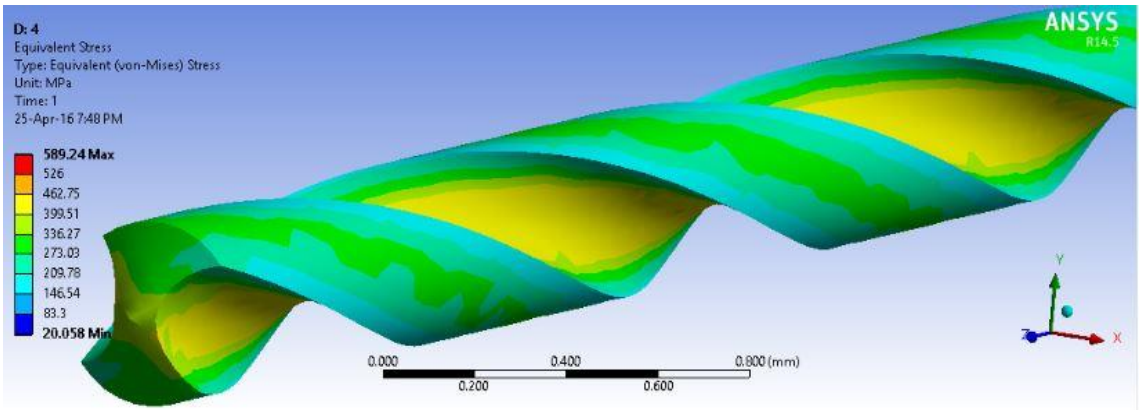

Fig. 4.12: Representative image of equivalent stress at condition (10000 rpm, 12µm/rev)

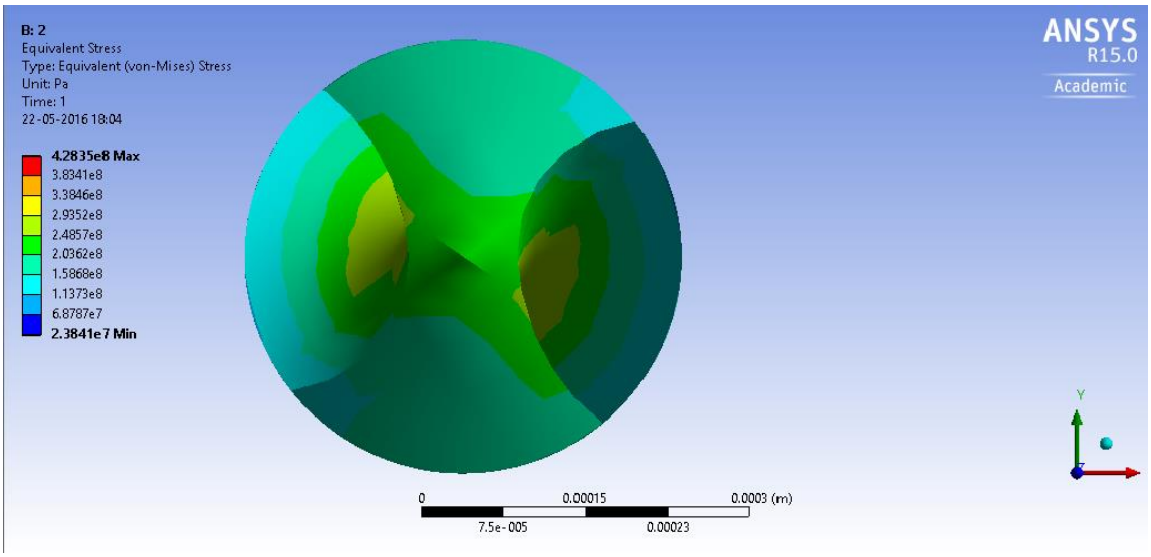

Fig. 4.13: Maximum principal stress in axial and diametric plane at condition (10000 rpm, 12µm/rev)

4.3 Surface integrity

4.3.1 Surface roughness

Owing to difficulty associated with the measurement of surface roughness of hole surface; attempt was made to determine the same at the bottom of the hole using a non contact 3-D surface profilometer. The surface roughness would primarily reveal the contribution of chisel edge since pilot hole was not drilled a prior. Since finite element simulation has demonstrated that the deformation and stress at and around chisel edge increased with cutting speed and feed, it is reasonable that they would have considerable effect on surface roughness measured at the bottom surface. Fig.4.14 depicts a representative image of the surface profile and the values of average surface roughness (R_a) were plotted in Fig.4.15 by using the tabulated value from Table. 4.3.

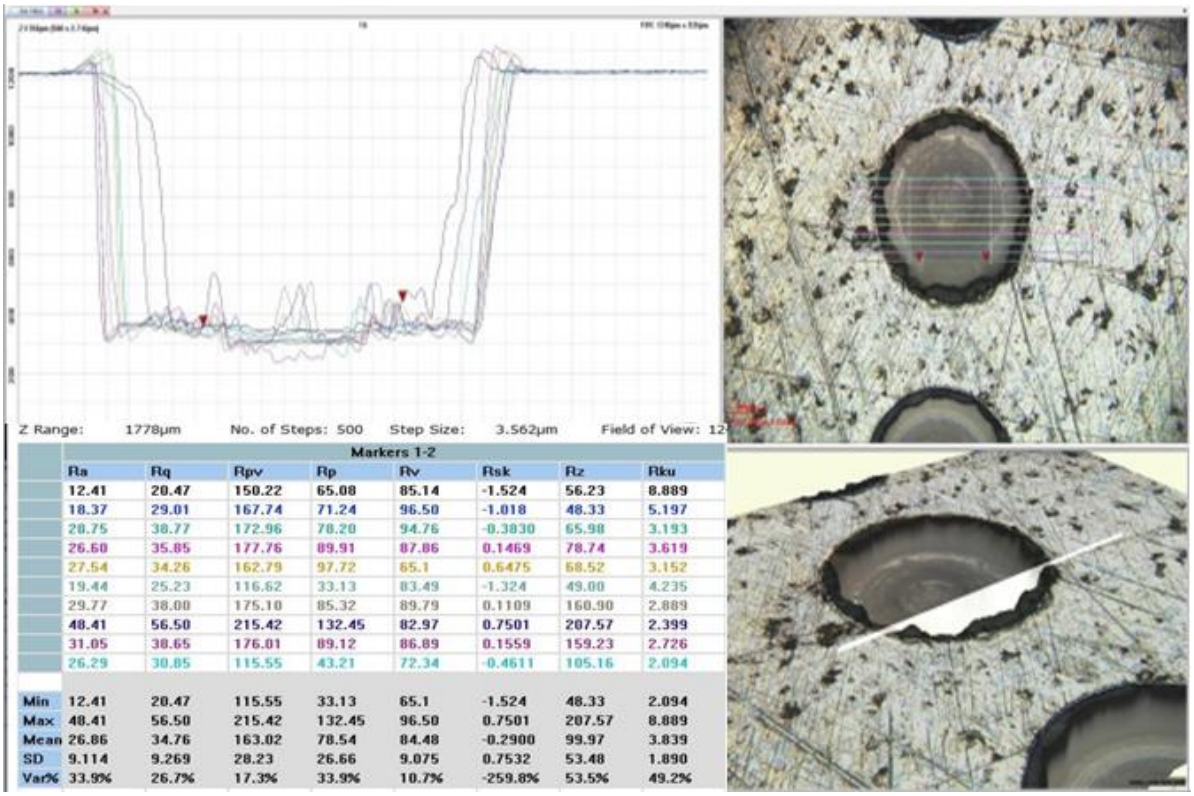

Markers 1-2

	Ra	Rq	Rpv	Rp	Rv	Rsk	Rz	Rku
	12.41	20.47	150.22	65.08	85.14	-1.524	56.23	8.889
	18.37	29.01	167.74	71.24	96.50	-1.018	48.33	5.197
	28.75	38.77	172.96	78.20	94.76	-0.3830	65.98	3.193
	26.60	35.85	177.76	89.91	87.86	0.1469	78.74	3.619
	27.54	34.26	162.79	97.72	65.1	0.6475	68.52	3.152
	19.44	25.23	116.62	33.13	83.49	-1.324	49.00	4.235
	29.77	38.00	175.10	85.32	89.79	0.1109	160.90	2.889
	48.41	56.50	215.42	132.45	82.97	0.7501	207.57	2.399
	31.05	38.65	176.01	89.12	86.89	0.1559	159.23	2.726
	26.29	30.85	115.55	43.21	72.34	-0.4611	105.16	2.094
Min	12.41	20.47	115.55	33.13	65.1	-1.524	48.33	2.094
Max	48.41	56.50	215.42	132.45	96.50	0.7501	207.57	8.889
Mean	26.86	34.76	163.02	78.54	84.48	-0.2900	99.97	3.839
SD	9.114	9.269	28.23	26.66	9.075	0.7532	53.48	1.890
Var%	33.9%	26.7%	17.3%	33.9%	10.7%	-259.8%	53.5%	49.2%

Fig. 4.14: Representative image of surface profile

Table.4.3: Surface roughness measurements for the micro holes

Hole No	N, rpm	f, µm/rev	Surface roughness(Ra), µm
1	10000	1	14.70
2	10000	4	31.85
3	10000	8	35.9
4	10000	12	31.5
5	20000	1	18.61
6	20000	4	23.15
7	20000	8	26.69
8	20000	12	36.2
9	30000	1	26.43
10	30000	4	35.82
11	30000	8	40.75
12	30000	12	46.47

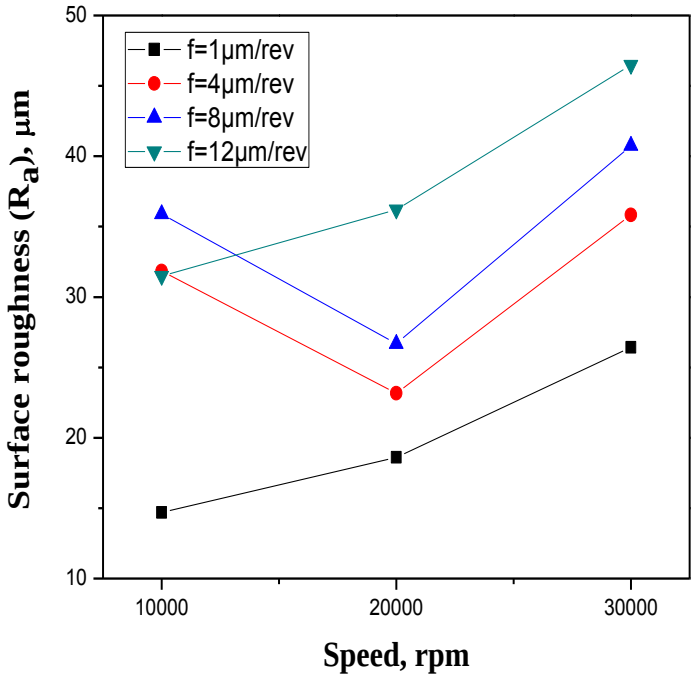

Fig. 4.15: Variation of surface roughness with speed rpm and feed rate

The trend clearly shows increasing trend in surface with both feed and cutting speed. While higher feed always produces rough surface, rising trend Ra with spindle speed might be attributed to high strain hardening tendency and consequent rise in deformation at the chisel edge as shown in Fig. 4.11.

4.3.2 Circumferential deformation layer

Careful investigation of the periphery of the micro holes clearly indicated formation of a deformed layer. These areas were magnified in order to measure their layer thickness and represented in Fig. 4.16.

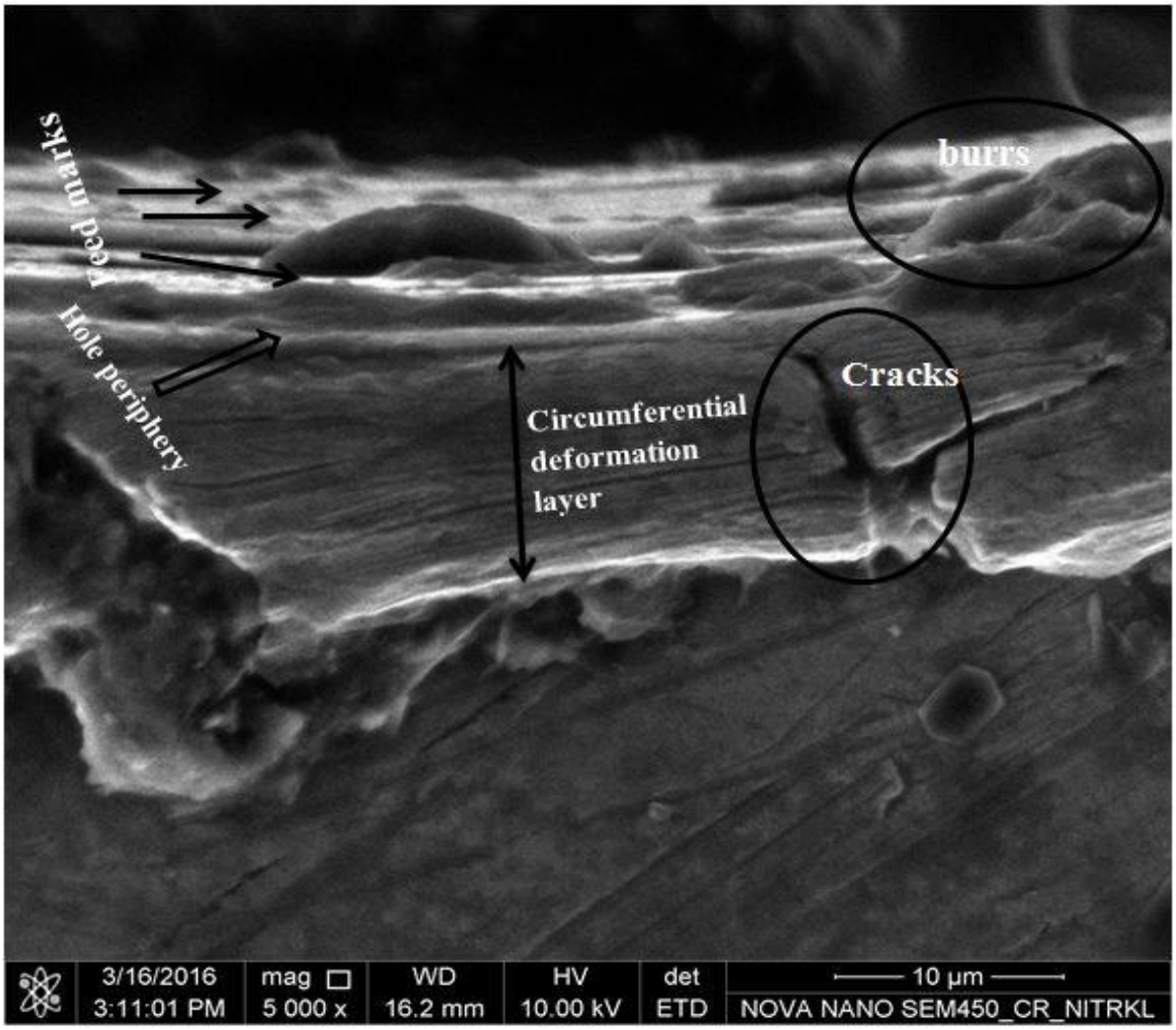

Fig. 4.16: Representative image circumferential deformation layer of drilled hole

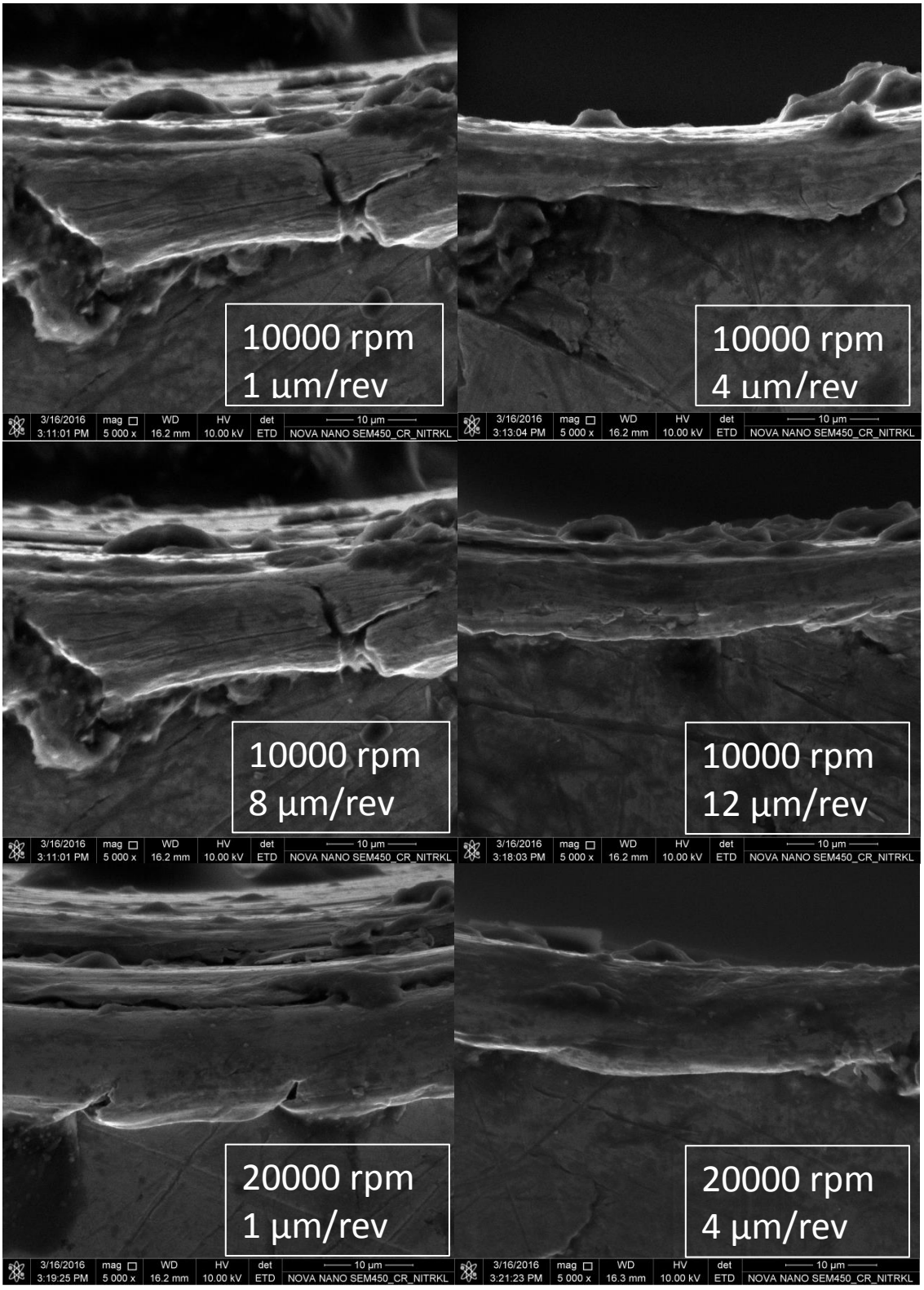
10000 rpm
1 µm/rev
3/16/2016 3:11:01 PM mag 5 000 x WD 16.2 mm HV 10.00 kV det ETD 10 µm NOVA NANO SEM450_CR_NITRKL
10000 rpm
4 µm/rev
3/16/2016 3:13:04 PM mag 5 000 x WD 16.2 mm HV 10.00 kV det ETD 10 µm NOVA NANO SEM450_CR_NITRKL
10000 rpm
8 µm/rev
3/16/2016 3:11:01 PM mag 5 000 x WD 16.2 mm HV 10.00 kV det ETD 10 µm NOVA NANO SEM450_CR_NITRKL
10000 rpm
12 µm/rev
3/16/2016 3:18:03 PM mag 5 000 x WD 16.2 mm HV 10.00 kV det ETD 10 µm NOVA NANO SEM450_CR_NITRKL
20000 rpm
1 µm/rev
3/16/2016 3:19:25 PM mag 5 000 x WD 16.2 mm HV 10.00 kV det ETD 10 µm NOVA NANO SEM450_CR_NITRKL
20000 rpm
4 µm/rev
3/16/2016 3:21:23 PM mag 5 000 x WD 16.3 mm HV 10.00 kV det ETD 10 µm NOVA NANO SEM450_CR_NITRKL

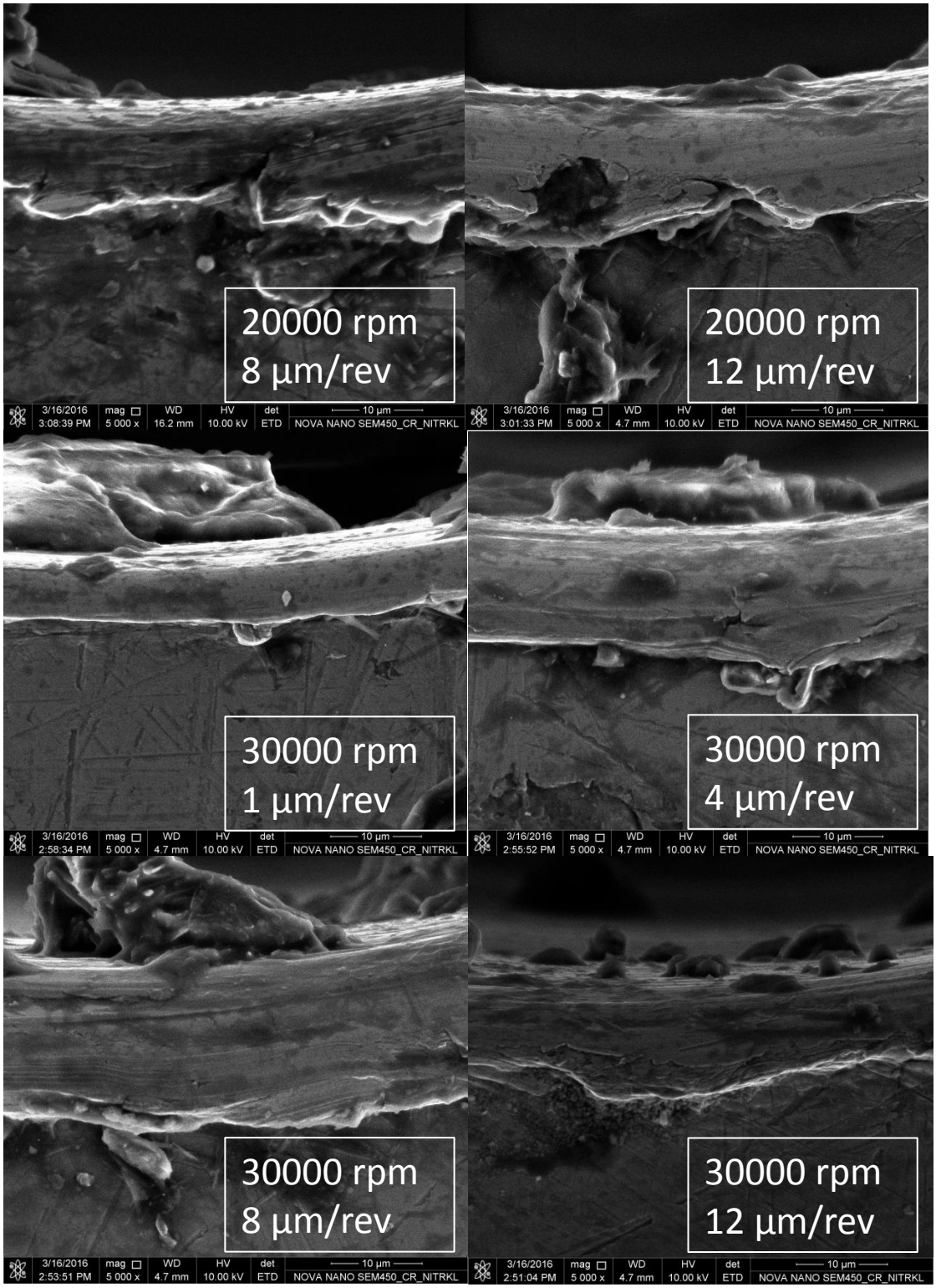

Fig. 4.17: Representative images of circumferential deformation layer with different conditions

Table.4.4: Measured circumferential deformation layer of micro drilling

Hole No	N, rpm	f, µm/rev	Circumferential deformation layer, µm
1	10000	1	6.18
2	10000	4	9.47
3	10000	8	9.84
4	10000	12	14.56
5	20000	1	7.96
6	20000	4	13.37
7	20000	8	15.74
8	20000	12	14.83
9	30000	1	8.49
10	30000	4	14.87
11	30000	8	13.69
12	30000	12	13.57

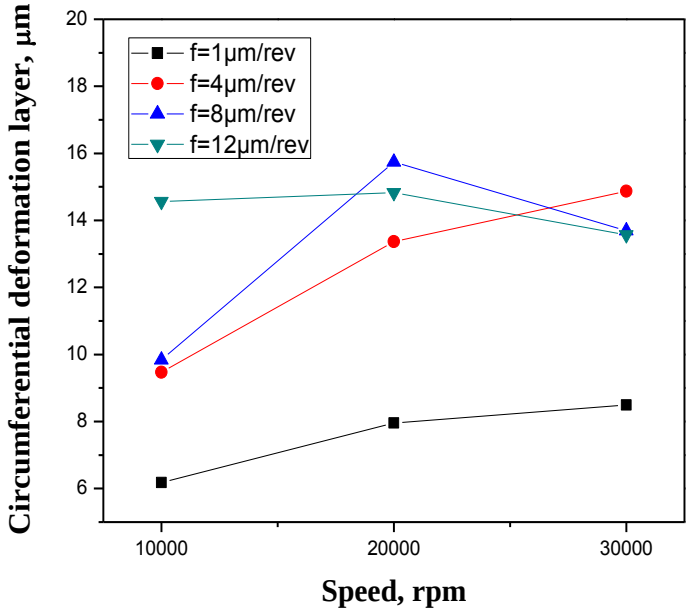

Fig. 4.18: Circumferential deformation layer with speed rpm and feed rate

According to the general trend obtained, it may be concluded that this deformed layer is a function of thrust force, radial forces, torque, temperature and in combination with strain hardening tendency of Incoloy 825 which were clearly influenced by feed and cutting speed. The formation of this layer can also be attributed to the elastic plastic deformation associated with micro machining process [16]. While deformation and high specific energy during micro machining have been discovered, pictorial evidence of such influence has been presented for the first time according to the best knowledge of the authors. It is believed that clear visibility of circumferential deformed layer is related to the tough work material like Incoloy 825 having strain hardening characteristics.

4.3.3 Oversize error of micro hole

It is known that radial runout causes radial forces, wandering motion of drill tip at the entrance of the hole [18]. During micro drilling of printed circuit board (PCB), radial runout was found which cause detrimental in the forms of hole enlargement, positional error and surface roughness [22]. It is therefore important to know how the cutting parameters influence the effects like enlargement of micro hole which is formed as oversize error of micro hole. This is obtained by subtracting diameter of fresh micro drill from the measured hole diameter. Fig. 4.20 shows FESEM images of the micro holes drilled under different cutting conditions. A magnified view of one such hole clearly indicating all the features including hole diameter is shown in Fig. 4.19.

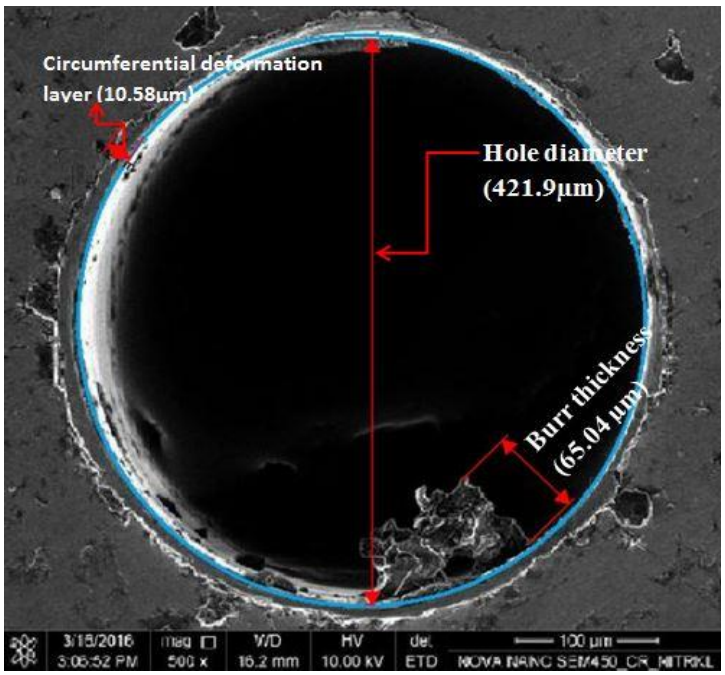

Fig. 4.19: Representative image of micro drilled hole

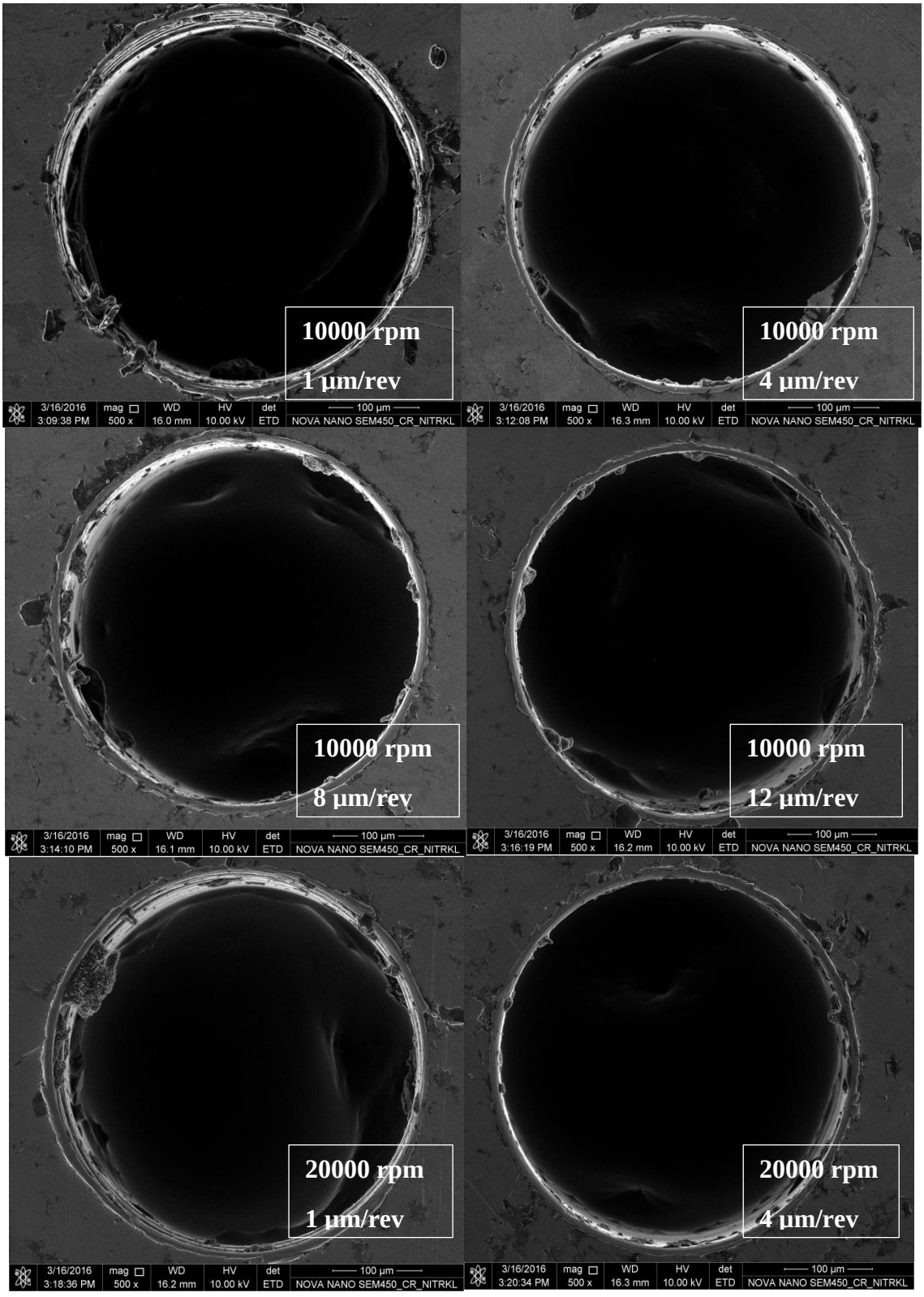
10000 rpm
1 µm/rev
3/16/2016 3:09:38 PM mag 500 x WD 16.0 mm HV 10.00 kV det ETD 100 µm NOVA NANO SEM450_CR_NITRKL
10000 rpm
4 µm/rev
3/16/2016 3:12:08 PM mag 500 x WD 16.3 mm HV 10.00 kV det ETD 100 µm NOVA NANO SEM450_CR_NITRKL
10000 rpm
8 µm/rev
3/16/2016 3:14:10 PM mag 500 x WD 16.1 mm HV 10.00 kV det ETD 100 µm NOVA NANO SEM450_CR_NITRKL
10000 rpm
12 µm/rev
3/16/2016 3:16:19 PM mag 500 x WD 16.2 mm HV 10.00 kV det ETD 100 µm NOVA NANO SEM450_CR_NITRKL
20000 rpm
1 µm/rev
3/16/2016 3:18:36 PM mag 500 x WD 16.2 mm HV 10.00 kV det ETD 100 µm NOVA NANO SEM450_CR_NITRKL
20000 rpm
4 µm/rev
3/16/2016 3:20:34 PM mag 500 x WD 16.3 mm HV 10.00 kV det ETD 100 µm NOVA NANO SEM450_CR_NITRKL

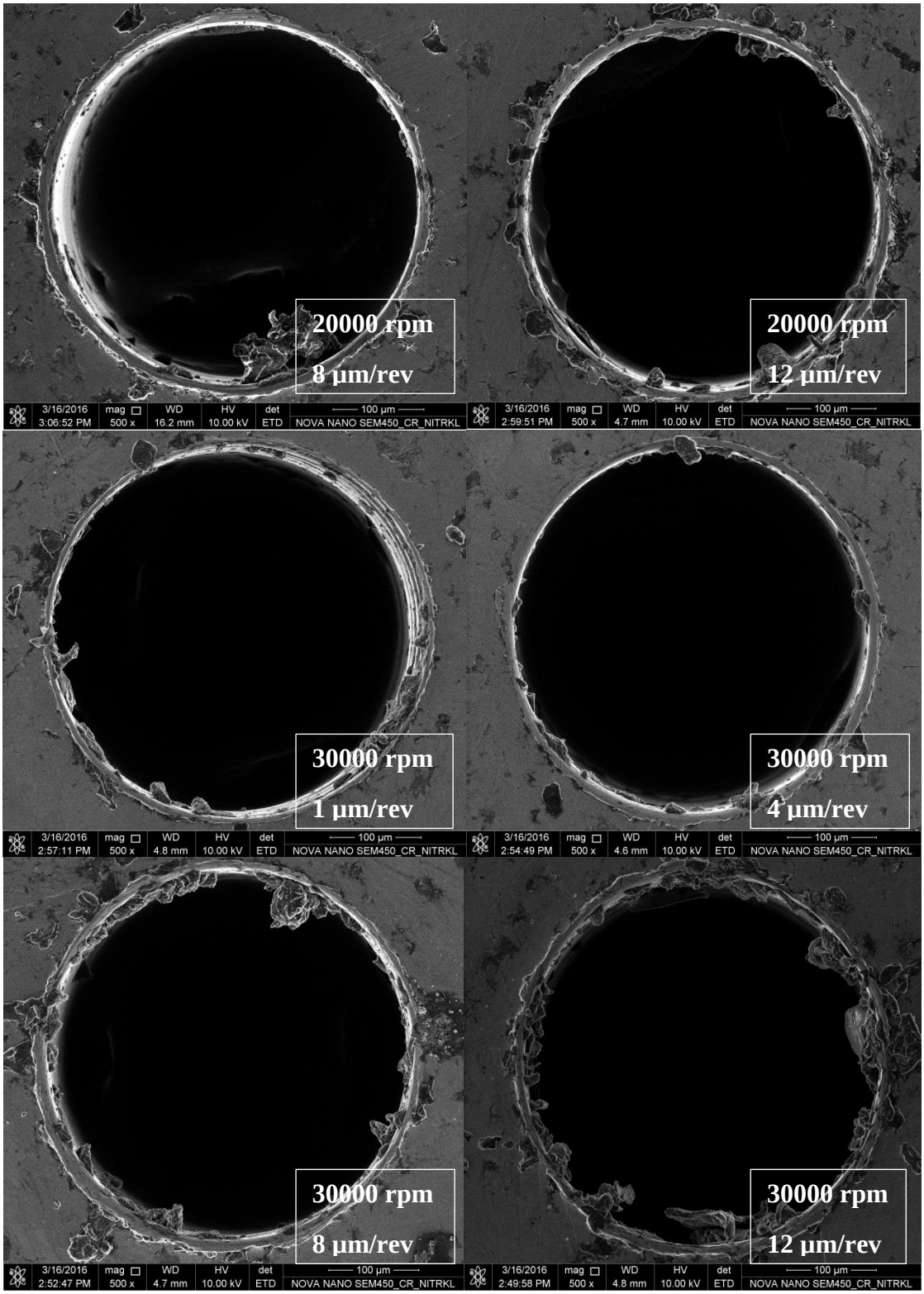

Fig. 4.20: Representative images of micro drilled hole with different conditions

The oversize errors of micro holes were thus calculated and plotted in Fig. 4.21 against both feed and spindle speed.

Table.4.5: Measured Oversize error of micro drilling

Hole No	N, rpm	f, µm/rev	Oversize error, µm
1	10000	1	38.7
2	10000	4	14.1
3	10000	8	19.3
4	10000	12	16.7
5	20000	1	30.9
6	20000	4	19.3
7	20000	8	21.9
8	20000	12	20.6
9	30000	1	27.0
10	30000	4	23.1
11	30000	8	25.7
12	30000	12	23.1

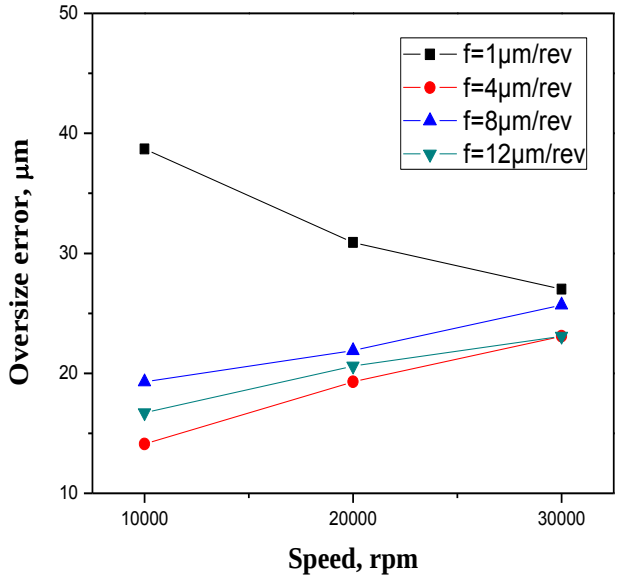

Fig. 4.21: Variation of oversize error with speed rpm and feed rate

Increasing trend of hole oversize with both feed and cutting speed might be explained with the result pertaining to thrust force, radial forces and torque. According to literature, radial runout also increases under high cutting parameters.

4.3.4 Investigation on white layer formation

Formation of white layer during machining Ni-based super alloy is a common occurrence due to expensive thermo-mechanical deformation. The same is, therefore, expected during micro machining as well, at best in a reduced scale. Owing to the difficulty of selecting the drilled hole along the axial plane, attempt was made to investigate the formation of white layer avail along the hoop direction. After polishing and etching the samples, the regions were distinctly visible, as demonstrated in Fig. 4.22 on the drilled surface. On the top of the drilled surface, thermo-mechanical deformation is maximum and it results in a thin layer consisting of fine grained structure which could not be resolved in high resolution FESEM. This region is called white layer which is indicated in Fig.4.22. The region (zone I) underneath white layer is a zone of severe plastic deformation which is zone II. It is interesting to note from Fig. 4.22, the deformed grains exhibit clear tendency to orient parallel to the white layer , the surface of the drilled hole. Moreover the direction of orientation is along that of cutting speed as shown in Fig. 4.22. It is worth to mention that high end characterization technique like Electron backscatter diffraction (EBSD) mapping carried out by Imran et al [5,8] revealed deformation of grains of zone II, after taking the cross-section of drilled hole (i.e. along feed direction). However similar pictorial evidence of grain orientation after micro machining has hardly been reported so far. It is also the direct consequence of high specific cutting force and specific cutting energy during micro machining compared to that of macro machining. Zone II is followed by bulk material (zone III) consisting primarily of undeformed grains. Fig. 4.16 shows the formation of different zones obtained under different condition of spindle speed and feed. Close investigation of the FESEM images in Fig. 4.16 would indicate that thickness of white layer significantly increases with cutting speed but smooth increase in white layer thickness with feed was only evident under the condition of highest spindle speed i.e. 30000 rpm (comparing to a cutting speed of 37.69 m/min). It might be explained by the fact that cutting temperature steadily increases with cutting speed and thermal induced deformation typically plays a dominant role in the formation of white layer [23, 24].

Feed, on the other hand, is more specifically responsible for the augmentation in mechanical induced plastic deformation. Little consideration would reveal that rise in feed causes not only an increase in the thickness of zone II, i.e. plastic deformation zone, but also more prominent orientation of the grains i.e. larger no. of grains oriented in the direction of cutting speed. Below Fig. 4.22 shows clearly the three different zone, thickness of white layer and orientation of deform grain.

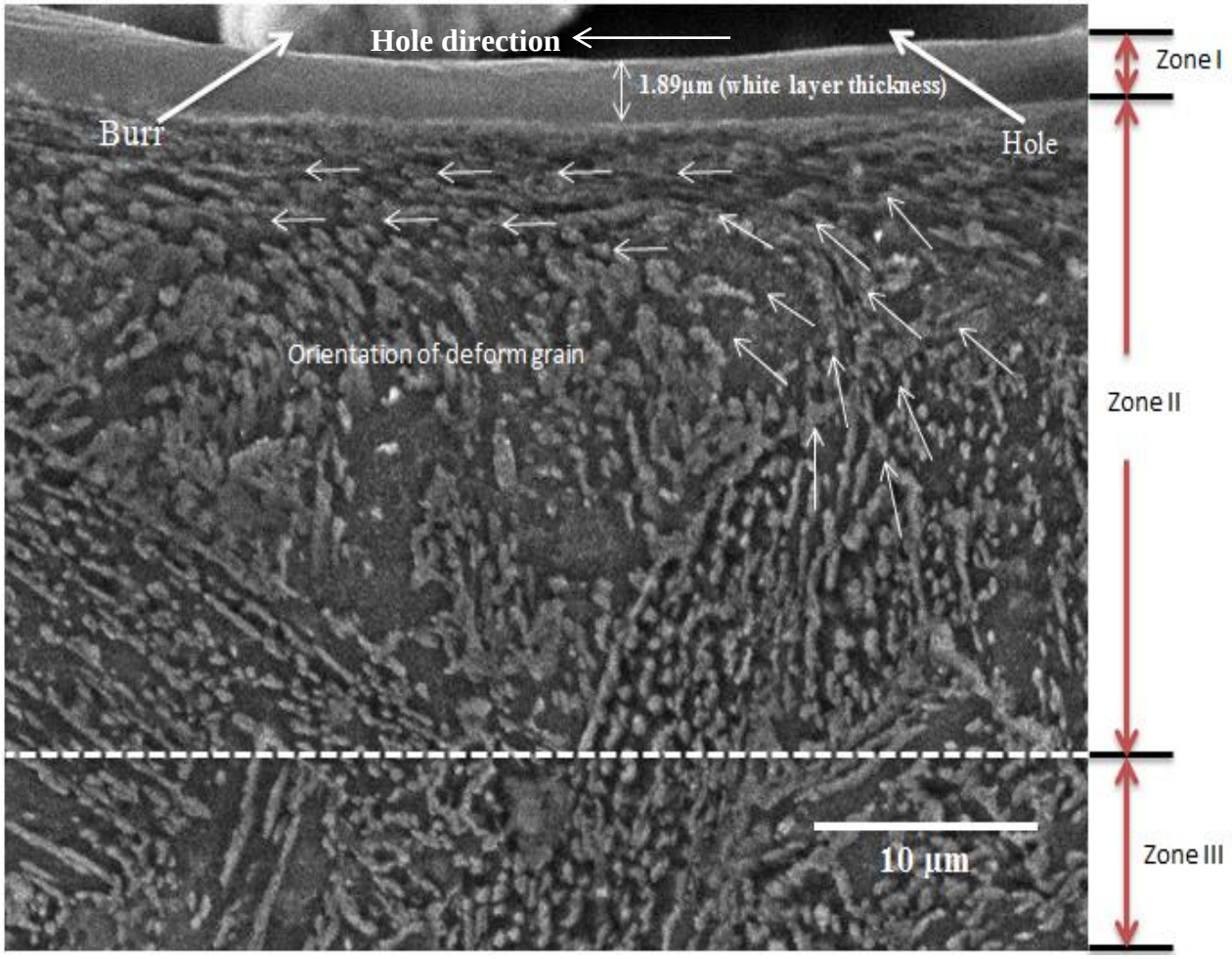

Fig. 4.22: Representative image of white layer

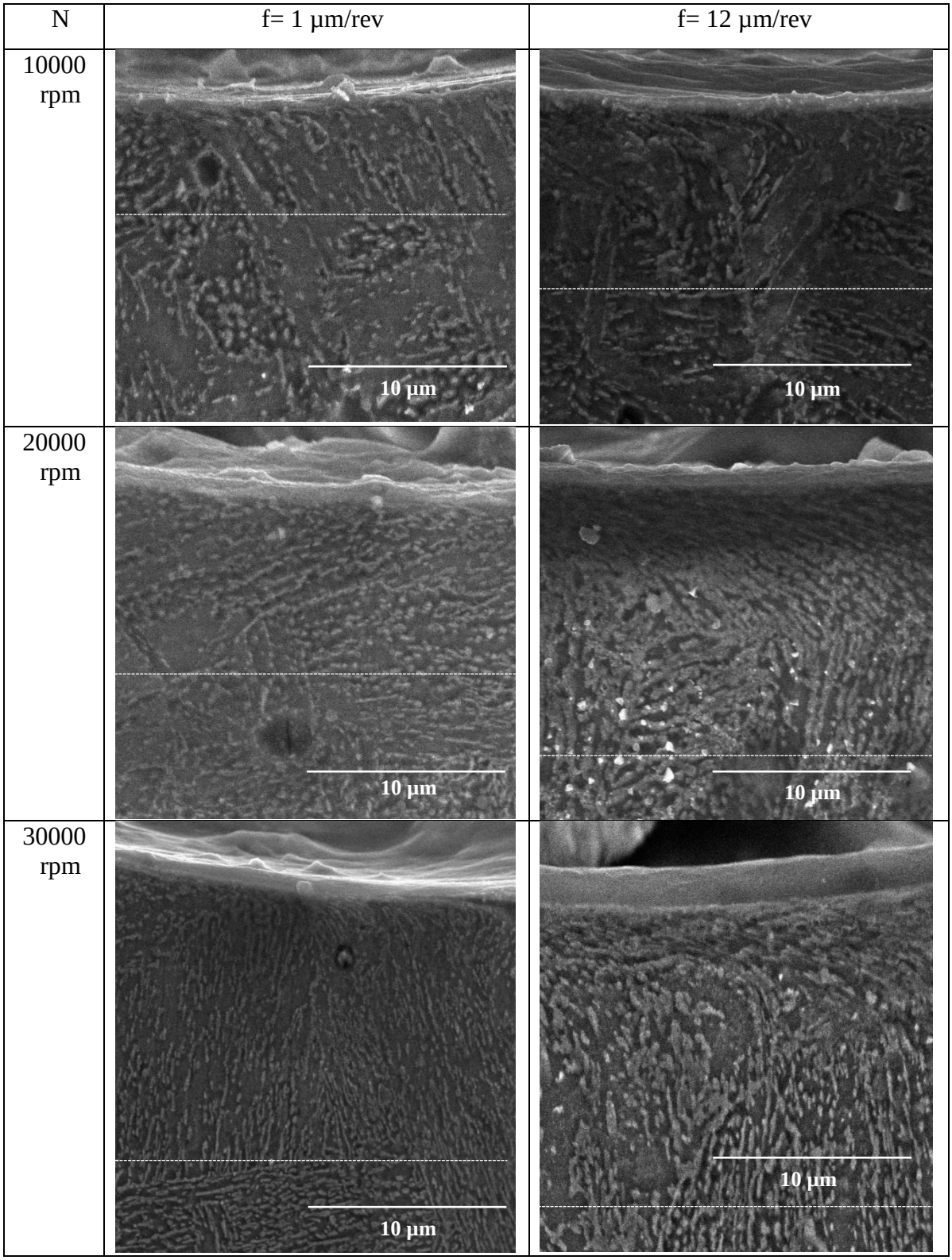

Fig. 4.23: Representative images of white layer at different speed rpm with lower and higher feed rate

4.4 Predictive regression models

By using the experimental values which are calculated by arithmetic mean are utilized for development of surface plots. Input parameters are speed and feed rate, and output responses are thrust force (F_z), radial forces i.e. F_x and F_y , torque, circumferential deformation layer, surface roughness and oversize error of micro hole. Comparatively analysis of different model carried out but in quadratic model found the significant with coefficient of determination (R^2). The quadratic regression equations are shown below

(a) **Thrust Force (F_z)** = 2.89926+6.51481E-005 * RPM+1.79031 * FEED -0.051214* $FEED^2$

(b) **Radial force (F_x)** = 0.16325-1.31780E-005* RPM-0.023759* FEED+ 5.63377E007* RPM * FEED +3.47665E-01* RPM^2+1.24787E-003* $FEED^2$

(c) **Radial force ($F_{y)}$** = +0.52636-4.36186E-005* RPM+0.014099* FEED+ 9.41329E-007* RPM * FEED+8.34826E-010* RPM^2-2.60779E-003 * $FEED^2$

(d) **Torque =** 0.14091-1.20670E-005* RPM-0.023847* FEED+7.62833E-007* RPM * FEED+2.55400E-010 * RPM^2+1.11789E-003 * $FEED^2$

(e) **Surface roughness (R_a)** = +34.66545-2.26200E-003 * RPM+1.54833* FEED + 6.76500E-008* RPM^2

(f) **Circumferential deformation layer (CDL) =** -3.71878+8.94227E-004 * RPM+1.89704* FEED-1.68964E-005* RPM * FEED -1.64125E-008* RPM^2-0.077693* $FEED^2$

(g) **Oversize error =** +40.37178-3.94091E-004* RPM-4.85124* FEED+ 6.48545E-005*RPM *FEED+2.87500E-009 * RPM^2+0.20886 * $FEED^2$

Effect of cutting speed and feed with different output responses are shown in Fig.4.24 to Fig.4.30 and also the predicted values are calculated shown in Table.4.6. When these predicted values are compared with statistical values, they show closed similarities. These predict values will be used for future research. Fig.4.26. shows some fluctuated values and proper trend with speed and feed rate. Fig.4.24. shows increasing trend with speed and feed.

Table.4.6: Predicted values of output responses

Hole No.	Speed, rpm	feed rate, µm/rev	Thrust force, N	Torque, N.mm	CDL, µm	SR, µm	Oversize dia (µm)	Radial force (F_x), N	Radial force(F_y) , N
1	10000	1	5.28983	0.030679	5.2326	20.3588	32.7245	0.04935	0.1945
2	10000	4	9.89255	-0.00121	9.2514	25.0038	23.2493	0.01370	0.2259
3	10000	8	14.5955	-0.01242	12.434	31.1971	16.4638	0.00109	0.1948
4	10000	12	17.6596	0.012132	13.131	37.3904	16.3618	0.02842	0.0802
5	20000	1	5.94131	-0.00574	9.0821	18.0338	30.2946	0.02751	0.0182
6	20000	4	10.5440	-0.01475	12.594	22.6788	22.7651	0.00875	0.0778
7	20000	8	15.2470	0.004552	15.101	28.8721	18.5738	0.01868	0.0844
8	20000	12	18.3111	0.059622	15.122	35.0654	21.066	0.06855	0.0075
9	30000	1	6.59279	0.008916	9.6492	29.2388	28.4398	0.07519	0.0088
10	30000	4	11.1955	0.022798	12.654	33.8838	22.8558	0.07334	0.0967
11	30000	8	15.8984	0.072609	14.485	40.0771	21.2587	0.10581	0.1409
12	30000	12	18.9626	0.158192	13.830	46.2704	26.3451	0.17821	0.1016

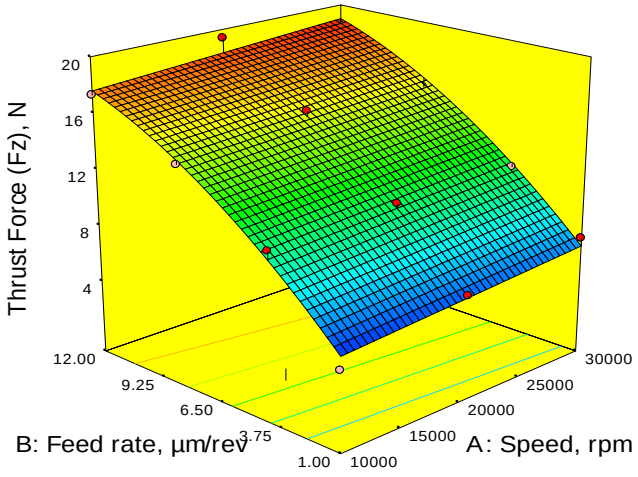

Workpiece material:	Incoloy 825
Tool material:	Cemented carbide
Cutting speed:	(10000,20000,30000) rpm
Feed rate:	(1, 4, 8, 12) µm/rev
Drill diameter:	0.4 mm
Drill depth:	1.25 mm

Fig.4.24: Effect of speed rpm and feed rate on thrust force (F_z)

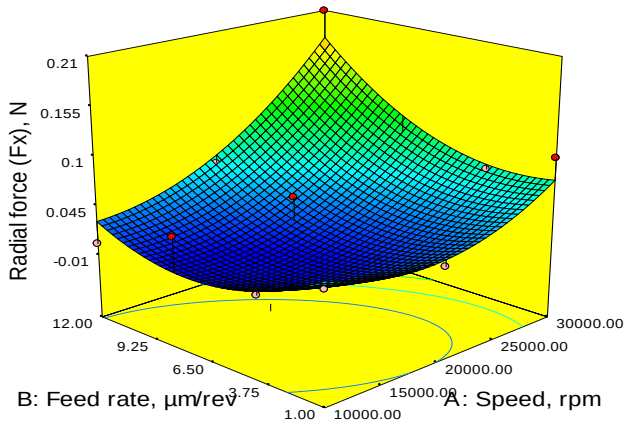

Workpiece material:	Incoloy 825
Tool material:	Cemented carbide
Cutting speed:	(10000,20000,30000) rpm
Feed rate:	(1, 4, 8, 12) µm/rev
Drill diameter:	0.4 mm
Drill depth:	1.25 mm

Fig.4.25: Effect of speed rpm and feed rate on radial force (F_x)

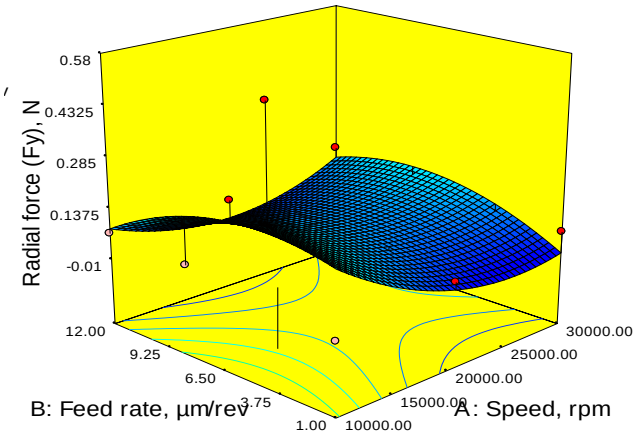

Workpiece material:	Incoloy 825
Tool material:	Cemented carbide
Cutting speed:	(10000,20000,30000) rpm
Feed rate:	(1, 4, 8, 12) µm/rev
Drill diameter:	0.4 mm
Drill depth:	1.25 mm

Fig.4.26: Effect of speed rpm and feed rate on radial force (F_y)

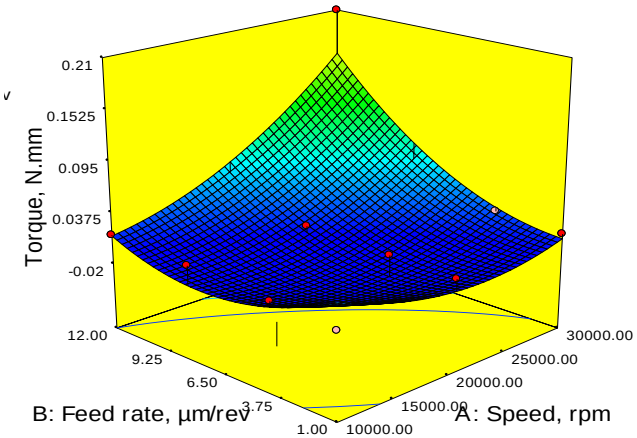

Workpiece material:	Incoloy 825
Tool material:	Cemented carbide
Cutting speed:	(10000,20000,30000) rpm
Feed rate:	(1, 4, 8, 12) µm/rev
Drill diameter:	0.4 mm
Drill depth:	1.25 mm

Fig.4.27: Effect of speed rpm and feed rate on torque

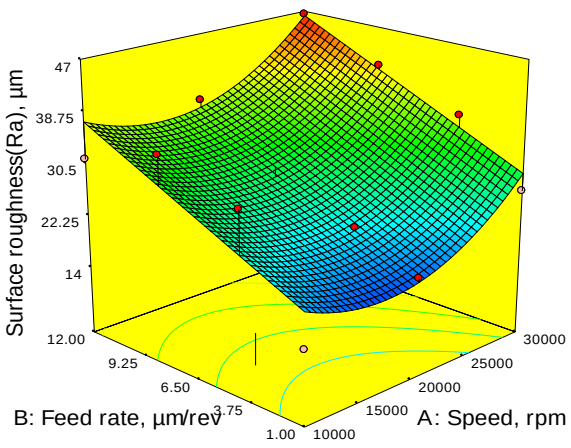

Workpiece material:	Incoloy 825
Tool material:	Cemented carbide
Cutting speed:	(10000,20000,30000) rpm
Feed rate:	(1, 4, 8, 12) µm/rev
Drill diameter:	0.4 mm
Drill depth:	1.25 mm

Fig.4.28: Effect of speed rpm and feed rate on surface roughness (R_a)

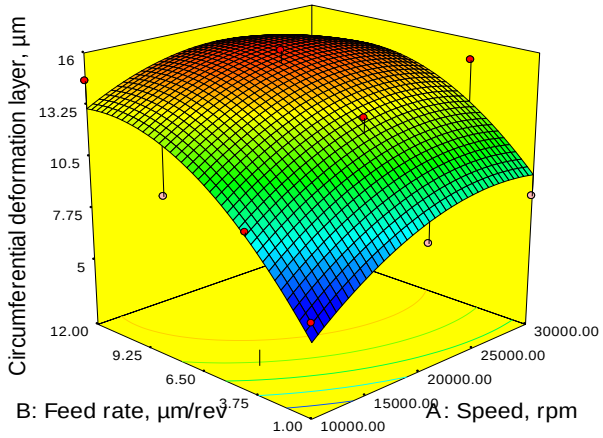

Workpiece material:	Incoloy 825
Tool material:	Cemented carbide
Cutting speed:	(10000,20000,30000) rpm
Feed rate:	(1, 4, 8, 12) µm/rev
Drill diameter:	0.4 mm
Drill depth:	1.25 mm

Fig.4.29: Effect of speed rpm and feed rate on circumferential deformation layer

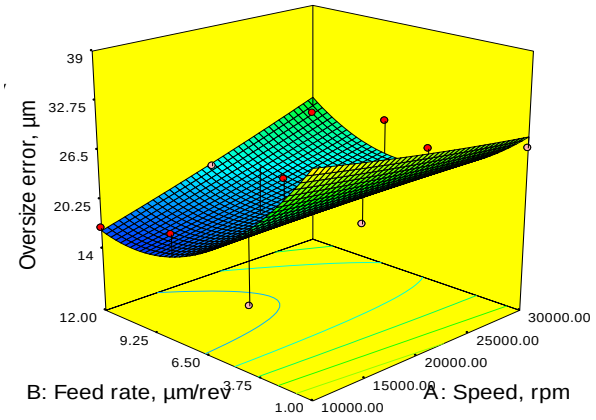

Workpiece material:	Incoloy 825
Tool material:	Cemented carbide
Cutting speed:	(10000,20000,30000) rpm
Feed rate:	(1, 4, 8, 12) µm/rev
Drill diameter:	0.4 mm
Drill depth:	1.25 mm

Fig.4.30: Effect of speed rpm and feed rate on oversize error

CHAPTER 5

Conclusions

The present research work investigated the influence of cutting parameters on various micro machining characteristics during micro drilling of Incoloy 825. The following conclusions are derived from the study.

1. Apart from expected increase in thrust force, radial forces and torque with feed, they showed rising trend with cutting speed as well. This was attributed to the prominent strain hardening effect of incoloy 825 which increases with cutting speed.
2. Surface roughness of the bottom surface of the micro hole also increased with both cutting speed and feed.
3. Even very small values of radial forces caused oversize error of micro hole which was the highest under lowest parameter combination. General trend, however showed increase in oversize error with speed as well as feed.
4. From the FE modeling it was concluded that deformation and equivalent stress in the micro drill not only increased with cutting parameters, but maximum values were obtained in and around the chisel edge.
5. The distinct zones were visible in the sub-surface region, when viewed along hoop direction. White layer increased with cutting parameters in the range of 1-2.8 μm. However, cutting speed clearly had greater influence on the formation of white layer than feed in micro drilling of Incoloy 825.
6. The study revealed the formation of plastic deformation zone (zone II) with clear sign of orientation of the deformed grains in the direction of cutting speed trying to align themselves parallel to the hole surface.
7. From the careful observation of all result, it can be overally concluded that optimal results in the form of superior dimensional accuracy, minimum circumferential damage, burr formation, minimum radial force, torque and reasonable less value of thrust force.

Future Scope of Work

- Effect of peck drilling and pilot hole (prior to actual drilling can also be investigated on micro drilling performance).
- Effect of coated micro tool can also be evaluated.

References

[1] I Rahamathullah and MS Shunmugam," Thrust and torque analyses for different strategies adapted in microdrilling of glass-fibre-reinforced plastic", DOI: 10.1243/09544054JEM2151.

[2] Jung Soo Nam, Pil-Ho Lee , Sang Won Lee," Experimental characterization of micro-drilling process using nanofluid minimum quantity lubrication", International Journal of Machine Tools & Manufacture 51 (2011) 649–652.

[3] Duck Whan Kim , Young Soo Lee , Min Soo Park , Chong Nam Chu ," Tool life improvement by peck drilling and thrust force monitoring during deep-micro-hole drilling of steel", International Journal of Machine Tools & Manufacture 49 (2009) 246–255.

[4] M Imran, P T Mativenga, S Kannan, and D Novovic, "An experimental investigation of deep-hole microdrillingcapability for a nickel-based superalloy", DOI: 10.1243/09544054JEM1217.

[5] Muhammad Imran , PaulT.Mativenga , AliGholinia, PhilipJ.Withers," Comparison of tool wear mechanisms and surface integrity for dry and wet micro-drilling of nickel-base superalloys", International JournalofMachineTools&Manufacture76(2014)49–60.

[6] Dong-Woo Kim , Myeong-Woo Cho, Tae-Il Seo and Eung-Sug Lee," Application of Design of Experiment Method for Thrust Force Minimization in Step-feed Micro Drilling", Sensors 2008, 8, 211-221.

[7] Lijuan Zheng , ChengyongWang, LipengYang , YuexianSong , LianyuFu," Characteristics of chip formation in the micro-drilling of multi-material sheets", International Journal of Machine Tools & Manufacture 52 (2012) 40–49.

[8] Muhammad Imran & Paul T. Mativenga & Ali Gholinia &Philip J. Withers," Evaluation of surface integrity in micro drilling process for nickel-based superalloy", Int J Adv Manuf Technol (2011) 55:465–476

[9] B.K. Hinds , G.M. Treanor," Analysis of stresses in micro-drills using the finite element method", International Journal of Machine Tools & Manufacture 40 (2000) 1443–1456.

[10] Gwo-Lianq Chern, Han-Jou Lee," Using workpiece vibration cutting for micro-drilling",Int J Adv Manuf Technol (2006) 27: 688–692.

[11] Hongyan Shi, Hui Li and Shengzhi Chen," Temperature simulation and its application in on-line temperature measurement of a micro drill bit", [DOI 10.1108/CW-10-2014-0045].

[12] M.M. Okasha, P.T. Mativenga, N. Driver, L. Li," Sequential laser and mechanical micro-drilling of Ni superalloy for aerospace application", CIRP Annals - Manufacturing Technology 59 (2010) 199–202.

[13] I Rahamathullah and MS Shunmugam," Analyses of forces and hole quality in micro-drilling of carbon fabric laminate composites", DOI: 10.1177/0021998312445594.

[14] S. Sahoo, A. Thakur & S. Gangopadhyay," Application of Analytical Simulation on Various Characteristics of Hole Quality during Micro-Drilling of Printed Circuit Board", DOI: 10.1080/10426914.2016.1140189.

[15] Karali Patra, Ravi Shankar Anand, Markus Steiner & Dirk Biermann," Experimental Analysis of Cutting Forces in Microdrilling of Austenitic Stainless Steel (X5CrNi18-10)", ISSN: 1042-6914 (Print) 1532-2475.

[16] Azlan Abdul Rahman, Azuddin Mamat, Abdullah Wagiman," Effect of Machining Parameters on Hole Quality of Micro Drilling for Brass",Volume 3,No-5,may 2009.

[17] H. Nakagawa , K. Ogawaa, A. Kihara, T. Hirogaki," Improvement of micro-drilled hole quality for printed wiring boards", Journal of Materials Processing Technology 191 (2007) 293–296.

[18] HidehitoWatanabe, Hideo Tsuzaka, Masami Masuda, "Microdrilling for printed circuit boards (PCBs)—Influence of radial run-out of microdrills on hole quality", Precision Engineering 32 (2008) 329–335.

[19] D. Biermann • M. Kirschner • D. Eberhardt," A novel method for chip formation analyses in deep hole drilling with small diameters", DOI 10.1007/s11740-014-0566-7.

[20] Irfan Ucun, Kubilay Aslantas, FevziBedir," An experimental investigation of the effect of coating material on tool wear in micro milling of Incoloy 718 super alloy", Wear 300 (2013) 8–19.

[21] C. K. Huang & C. W. Liao & A. P. Huang & Y. S. Tarng,"An automatic optical inspection of drill point defects for micro-drilling", Int J Adv Manuf Technol (2008) 37:1133–1145.

[22] Osamu HORIUCHI, Masami MASUDA and Takayuki SHIBATA," Bending of Drill and Radial Forces in Micro Drilling", *Advanced Materials Research Vol. 797 (2013) pp 642-648.*

[23] A.Thakur, S.Gangopadhyay, K.P.Maity," Effect of cutting speed and tool coating on machined surface integrity of Ni-based super alloy", Procedia CIRP 14 (2014) 541 – 545.

[24] A. Thakur, A. Mohanty, S. Gangopadhyay," Comparative study of surface integrity aspects of Incoloy 825 during machining with uncoated and CVD multilayer coated inserts", Applied Surface Science 320 (2014) 829–837.